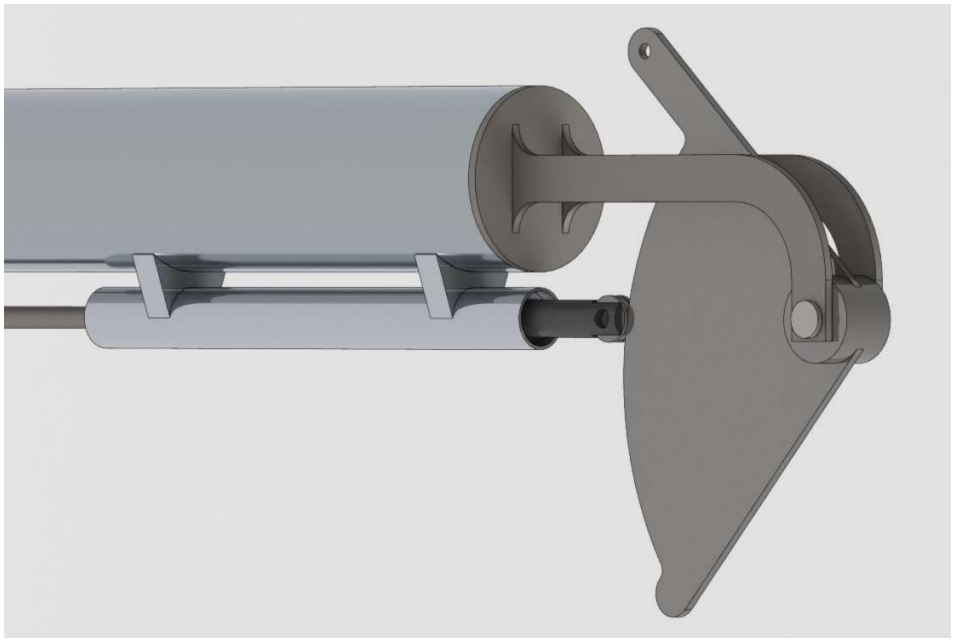

Design of a flight-control system for foiling dinghies with a T-wing and individual flaps.

Bachelor thesis in Mechanical construction engineering

Albin Boman

Department of mechanics and maritime sciences

CHALMERS TEKNISKA HÖGSKOLA
Göteborg, 2020
www.chalmers.se

Department of mechanics and maritime sciences
CHALMERS TEKNISKA HÖGSKOLA
Göteborg, Sverige 2020
www.chalmers.se

Bachelor thesis for the bachelor program in mechanical engineering at
Chalmers University of Technology

CHALMERS

A concept development report of a foil control system for a sailing two-man dinghy.

Supervisor: Lars Larsson
Examiner: Per Hogström

Preface

In this report a concept development project is presented, which addresses the aspects arising in the development of a product to be implemented in an existing environment of constraints and demands.

Thanks to the Chalmers Formula Sailing project and Lars Larsson for the opportunity to assist in the development of a sailing craft of the future. Extra thanks to Nimal Sudhan Saravana Prabahar, who assisted in understanding the problem and the limitations of the existing design.

Abstract

Sailboats and dinghies have been ”foiling” for a long time now, but they all face the same problems with stability when losing the righting moment of the hull when it leaves the water. Chalmers Formula Sailing team’s idea to use split flaps, which can be used to control the centre of lift is a new way to tackle this problem. This report investigates possible concepts for controlling a split flap system mechanically.

The proposed solution to this problem is a linkage system transferring a signal from the water surface to the flap of the foil to control the height at which the boat flies. It includes an axial cam which can be customized to enhance the foiling performance of the boat with respect to both stability and speed. This solution shows significant improvements compared to the concept previously suggested to Formula Sailing. This report shows that a split flap system can be controlled in many ways with benefits and deficits to each concept, however the concept suggested is the best option with respect to performance, durability and adjustability.

The outcome gives a clear picture of how this concept can be implemented into the existing design with important design features pointed out. Further work will include engineering on other areas to complete the full concept, such as hydrodynamics and structures of the foil itself.

Important delimitations have been made regarding the detail level of the parts included in the system, detailed fatigue calculations and economical aspects.

Keywords: foiling, dinghy, Formula Sailing, split-flap, control-system, finite element analysis, cam, concept development, sailing.

Contents

List of variables

M_{in} - Input torque at sensor

M_{out} – Required torque at flap

F_{in} – Force acting on sensor

F_{out} – Force acting on flap

L_w – Lever length of force acting on the sensor

L_f – Lever length of force acting on the flap

M_{max} – Maximum torque at flap

α_f – Flap angle

H – Ride height

$H_2 -$ Ride height redefined

α_{opt} – Optimal flap angle

α_w – Wand angle

$\alpha_c -$ Cam slope angle

$dr -$ Change in cam radius

$r -$ Base radius of cam

$x -$ Vertical movement of the flap lever

1 Introduction

In November 2016 Chalmers was invited to participate in 1001Vela Cup for the first time. This is a student competition where the participants design, build and sail an extreme two-person dinghy, also known as "Skiff". The boats are limited by a very simple class rule, where only length, beam, and sail area are limited. However, the hull must be made from at least 70% organic material. The following year Formula sailing was formed to design and build a boat to compete in the 2018 issue of the 1001Vela Cup. The result, Linnea, was a design like no other, the hull was made of a renewable composite consisting of lflax fibers, bio-epoxy and a core of balsa. The boat was fast enough to win the regatta by winning almost all races. For the 2019 issue, the team was confident that the competition hadn't caught up yet and only some minor changes were made on the boat.

The organic material rule has up until this year also included any foils attached to the hull, but now exotic materials are allowed on the boat's centreboard and rudder, allowing foils with much greater strength. This, in turn, allows for some even more extreme design solutions to the boat. By mounting horizontal foils on the end of each vertical foil a lifting force can be produced, lifting the boat out of the water significantly reducing the hydrodynamic drag on the boat. This is also known as foiling.

In the aftermath of the success in 2018 Formula sailing now considered the idea of making Linnea foil, and the Bachelor's thesis *En flygande kappseglingsjolle* (Dackhammar et al, 2018) examined this thoroughly with the conclusion that it indeed will be possible. This thesis mostly focused on the hydrodynamics and strength issues involved in this design but didn't consider how to control the flight in any deep analysis.

1.1 Background

Foiling has been a proven concept on dinghies for around 20 years (Bethwaite, 2008), it started in the early 2000s in the development class International Moth. John Ilett and his brother spent several years trying to get their dinghy to fly, and the result was a "T" foil with an adjustable flap on the trailing edge like an airplane wing. The flap is continuously controlled by a fly-height measurer. Since then, Moths have been flying. The last two editions of the Americas Cup have been held on foiling catamarans and in 2021 it will be sailed by foiling monohulls. Even the offshore racers are now foiling far out at sea. The reason for this foiling trend is simply because it is faster, for as long as you can control it.

A new idea to make foiling more controlled was investigated by Formula Sailing in the thesis (Dackhammar et al, 2018). The concept idea is to increase control of the boat by adjusting each side of the flap individually depending on the distance of each side to the water surface. This would make the foil provide a greater lifting force on the side to which it is heeled, resulting in a righting force which would make the flight more controllable for the sailor.

Previous publications, and existing research made by or for the Formula Sailing including (Dackhammar et al, 2018) and *Chalmers Formula Sailing High-Performance Skiff* (Acerbi, et al., 2017) will be the basis for this thesis, especially the work done by Nimal Prabahar (Prabahar, 2020) which shows an in-detail simulation on how Linnea will have to be configured to fly. Present work will be a more specific study on how to mechanically control flight using previous research. The focus in this study will be on the mechanical control system, no hydrodynamic changes will be made to the existing foils or the boat. There are some calculations, theories, and models in previous designs of Linnea that will be considered during this project.

1.2 Aim of the thesis

The purpose of the thesis is to develop and design a concept of a mechanical control system that allows full use of the split-flap foil configuration, meeting the criteria set by Formula Sailing's Velocity prediction program calculations.

The focus will lie in designing an accurate and reliable system that will provide the performance asked upon by formula sailing and its sailors. The system should also be easy to use to not complicate the sailing experience.

1.3 Limitations

This thesis will only consider a control system for the main foil on the existing Formula Sailing boat Linnea and will thereby be limited from considering the system on other boats. Figure 1.1 shows a 3D render of Linnea in a non-foiling configuration. The system will be designed to meet the foiling dynamic demands set by Formula Sailing. Limitations on materials and dimensions used are stated by the 1001Vela Cup rules (1001Vela Cup, 2019). Because of the 70% organic material rule, organic materials should be used where possible. However, the functionality of the system should not be compromised by this. Since the system will be used in saltwater all metal parts should be made of "stainless steel". No further investigation in material selection will be made

This thesis will not consider hydrodynamics of the foils or sensors, only the mechanics involved in the control system. The control system will only adjust the main foil and not the rudder foil. No regard to the economics of the concepts will be considered.

Figure 1.1 3D Render of Formula Sailing's sailboat Linnea in her current state.

The project will only develop a theoretical concept to be implemented on the boat until the 2020 edition of the 1001Vela Cup. No actual construction or building of parts will be completed during this project, but future projects will be able to implement the design made.

The forces acting on the foils and the system is given by Formula Sailing's calculations on Linnea. The system will be designed to withstand the most extreme forces put on the system even at failure in other parts of the boat.

From a sailor's point of view the system needs to be easy to control and adjust while sailing to enable adjustments to changing conditions or styles of sailing. It also needs to be reliable and provide a safe feeling for the sailors to not hinder them in their work physically and mentally. (Boman, 2019)

2 Theoretical reference

The basic theory of sailing will apply in a lot of calculations of this project, as well as basic calculations of forces and torques.

All the dimensions and characteristics of Linnea is provided by Formula Sailing and the report (Acerbi, et al., 2017). The basic dimensions are stated in Table 1

Table 1 Dimensions of Linnea (Acerbi, et al., 2017)

Length Over All	4600 mm	Beam Over All	2095 mm
Hull draft	171 mm	Total draft	1702 mm
Length waterline	4600 mm	Beam waterline	954 mm
Displacement	250 kg	Total sail area	33 ^2

2.1 Basics of foiling

The theory behind foiling dinghies is simple: horizontal wings are mounted to the end of a dinghy's centreboard and rudder and with building speed these wings provide lift. Eventually, enough lift is generated to lift the boat out of the water, significantly reducing the resistance through removing the resistance of the hull altogether. Figure 2.1 shows the forces acting on the boat with a foiling configuration.

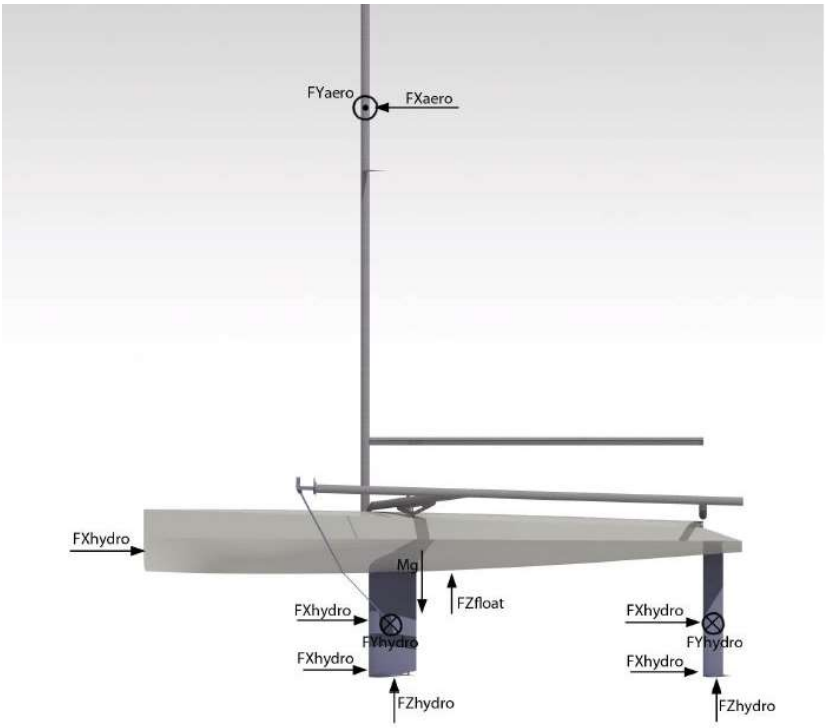

Figure 2.1 Sideview of Linnea including the forces acting on her during foiling to give an understanding of what it takes to foil. (Dackhammar et al, 2018)

To get out of the water is easy, the hard part is to stay in flight. To do so a control system is implemented on the main foil. The control system should automatically adjust the lift provided by the main foil depending on the fly height. This is done by changing the angle of a flap on the trailing edge of the foil. Figure 2.2 shows a section of the horizontal foil with two different settings of the flap, 0 and 10 degrees. The profile is a NACA 63-412.

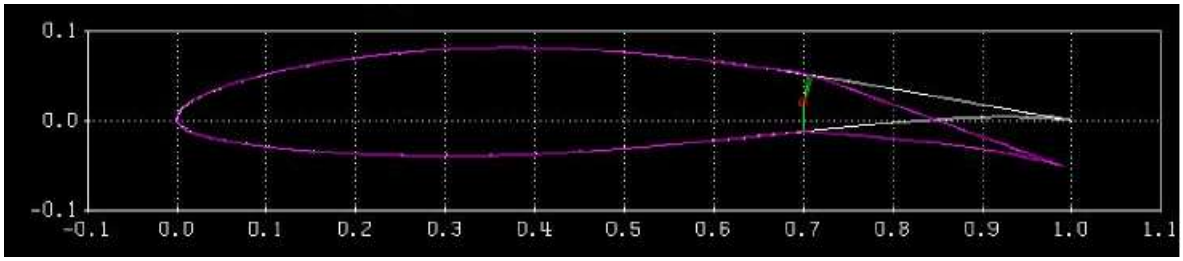

Figure 2.2 Section of the horizontal foil with two different flap angles. (Dackhammar et al, 2018)

2.2 Linnea's dimensions

The foil dimensions are further described in figure 2.3 and are developed by Formula sailing to enable Linnea to foil. Figure 2.3 shows one side of the foil area with the trailing edge flap dimensions shown.

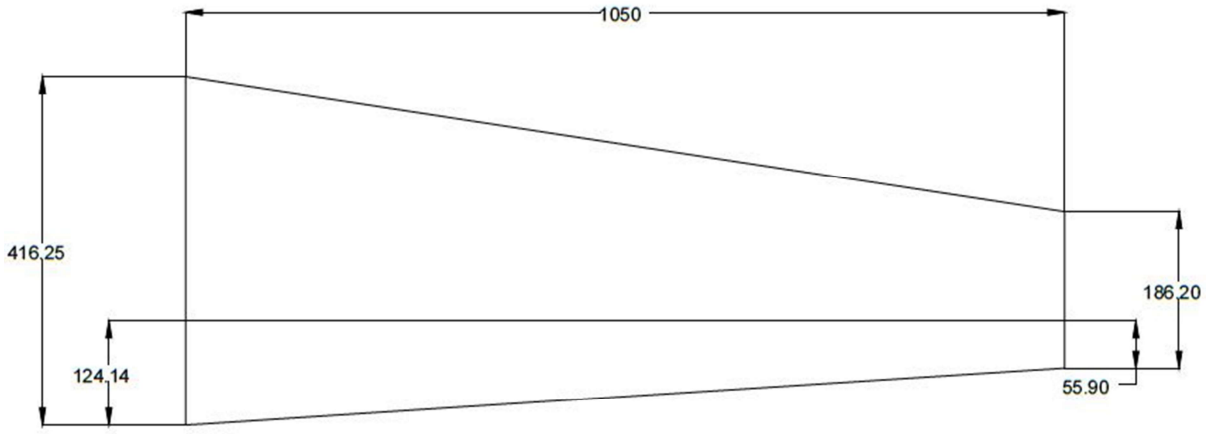

Figure 2.3 Top view of one side of the horizontal main foil to be fitted on Linnea

The force required to move the flap is provided by a "sensor". In most cases "wands" are used, which obtain the force by planing on the water. The force is transferred by the control system to the flap. These forces are turned in to torques by using the length of the force's levers. The variables are shown in figure 2.4.

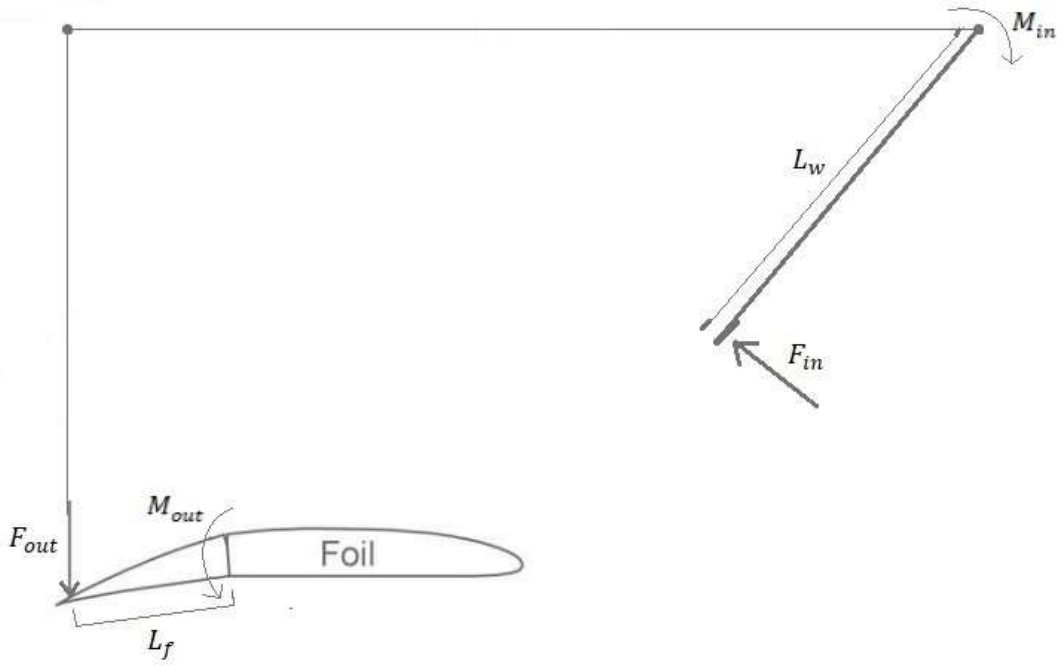

Figure 2.4 Exposure of forces acting on a classic control system. To the right is the input sensor (wand) which pivots depending of the boat height above the water. The signal is then transferred to the flap.

When the system is dynamic, friction forces must be taken in account. These will counteract the input signal increasing the input force needed to move the flap. The aim is to make F_{in} as small as possible since it will decrease hydrodynamic drag. This is done by reducing friction in the system and lengthening the levers as much as possible.

The maximum amount of output torque needed at the flap has been calculated by Prabahar (Prabahar, 2020) to $M_{max} = 30.45\ Nm$ per flap. This is a result of the maximum amount of lift ever put on the foil and the portion of that provided by the flap. On some rare occasions, the system will experience negative torques at the foil (Larsson, 2019).

The flap angle (α_f) will be in the range +4 to -7 degrees for stable flight without any heel, but the flap can be adjusted from +7 to -10 degrees. The system can be tuned to achieve a certain flap angle at a certain wand angle, allowing the vessel to fly stably.

2.3 Individual flaps

The individual flap concept was developed by Formula Sailing to make foiling more controlled for beginners. In theory, the flap of the main foil would be divided into two, one port and one starboard flap. The flaps would be operating individually depending on each side of the boat's distance to the water. This would provide more lifting force on the side the boat heels to, creating a righting moment and stabilizing the boat. This idea was born as sailors faced great problems with balance trying to fly Chalmers foiling Optimist (Larsson, 2019). To have two flaps acting individually would give the boat extra righting moment when the boat is heeling

as the centre of lift is moved to the leeward side of the foil. Figure 2.5 shows how the centre of lift is moved to the side of the foil when the boat is heeling due to the difference in flap angle increasing the lever to the centre of mass.

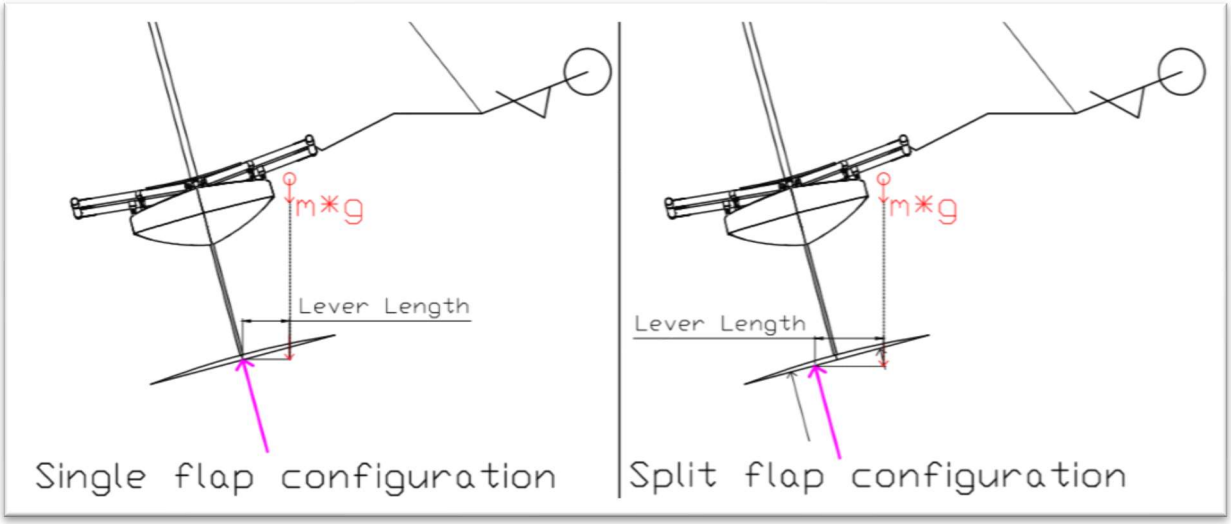

Figure 2.5 Difference in forces provided by a foil with individual flaps at heel compared to a single flap foil. Figure shows that the lever on which the mass works is lengthened with a split flap, and therefore increased righting moment is induced.

The big issue that Formula Sailing faced with this concept is that preferred lift for each side is not directly proportional to the ride height with a classic wand system, meaning that if the boat heels over and too much lift is moved to one side the total lift might not be enough to keep the boat above the water. This was mostly the case when heel dependent settings where tried out or other nonlinear behavior. Therefore, the team chose to aim for a linear approach to decrease the complexity of the design and of the control system. Then the same amount of lift that is added to one side when heeling is removed from the other, keeping the same total lift for that average ride height.

The optimal foil behavior is designed by Prabahar (Prabahar, 2020) and given by equation 1. It gives a flap angle $\boldsymbol{\alpha_f}$ depending on the ride height H which is the output and input for the control system.

$$\boldsymbol{\alpha_f = -11.9 * H + \alpha_{opt}} \qquad \textbf{(1)}$$

α_{opt} is set to 2 degrees, for the average conditions to expect in Palermo during the Vela Cup. If the wind speed is higher the optimal flap angle will change, and the system will need another pre-set. In Figure 2.6 this function plotted to show the linear behaviour needed for the system.

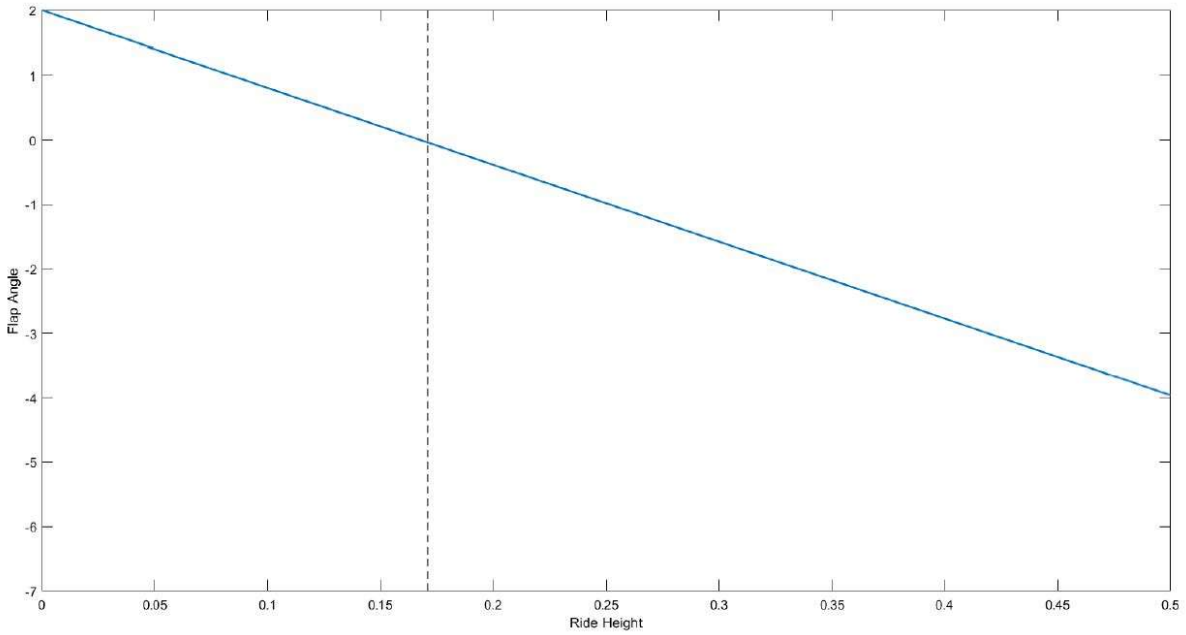

Figure 2.6 Ride height versus flap angle. Plotted line represents optimal angle for each flap.

In this plot the actual ride height is measured from -0,175 m below the water surface. This is the hull draft at zero speed. The dotted line in figure 2.6 represents the height when the boat is just flying, at a height of 0,175 m. The function is linear up to the maximum ride height of 0,5 m.

Another possibility provided by the individual flap system is the ability to change the center of lift even when the boat is not heeling. If a portion of the lift is moved to the leeward flap and the same amount removed from the windward, the center of lift is moved to leeward keeping the same amount of total lift. This is considered "performance mode" and can be made possible by up to 6 degrees of flap angle difference between the sides. If the mean angle follows the plot in figure 2.6 the boat has the same amount of total lift.

2.4 Strength calculations

Apart from the basic mechanical calculations required, the system will be dimensioned to save as much weight as possible without sacrificing strength and reliability. Beam bending, buckling and deformation will be calculated with elemental cases from (Dahlberg, 2001). The strength integrity will also be calculated with the standards set by Dahlberg.

Beam section modulus of a rectangular beam

$$W_b = \frac{M}{\sigma_b} = \frac{b*h^2}{6} \qquad \textbf{(2)}$$

Where W_b is the section modulus, M the torque on the beam and σ_b is the maximum stress of the cross section under bending load.

Definition of normal stress

$$\sigma = \frac{N}{A} \qquad \textbf{(3)}$$

Where σ is the stress in the material, N is the force normal to the surface and A is the cross-sectional area.

Bending of fixed beams

$$w(x) = \frac{PL^3}{6EI}(3\frac{x^2}{L^2} - \frac{x^3}{L^3}) \quad \textbf{(4)}$$

Where w is the bending deformation of the beam, P the force, L the length of the beam, E Young's modulus, I the moment of inertia and x the distance from the fixed point where w is measured.

Buckling of beams

$$P_s = \frac{\pi^2 EI}{L^2} \quad \textbf{(5)}$$

Where P_s is the critical force where the beam buckles, and I the moment of inertia.

Definition of max. shear forces

$$\tau_{tp} = \mu * \frac{T}{A} \quad \textbf{(6)}$$

Where μ is Jouravski factor, T the shear force and A the cross sectional area.

Calculations in this report also includes computerized finite element method analysis (FEM) based on the knowledge obtained from courses given on Chalmers based on the book *Finite Element Method, Its Basis & Fundamentals* (Zienkiewicz, C. Taylor, & L. Zhu, 1991)

2.5 Material data

The material data used throughout the thesis are presented in table 2

Table 2 Characteristics of stainless steel (Dahlberg, 2001). *And Flax fibre composites* (Libo, Nawawi, & Krishnan, 2013)

Material	Youngsmodulus (E)	Yield strength σ_s	Tensile strength σ_b
Standard Stainless steel	195 GPa	200 MPa	490 MPa
Flax Fibre Composite	20 ±2 GPa	-	260 MPa

Material data for Flax fibre composite properties varies a lot depending on its quality and composition. Average values where used for these applications.

2.6 Concept development

To develop a concept, different solutions can be gathered and put together, but to evaluate existing concepts and new ideas scientifically the report uses the Pugh-method (Pugh, 1990). It includes an evaluation matrix which ranks alternative solutions or parts of a concept to each other with respect to different design criteria.

3 Disposition

The report is divided into eight chapters. The beginning of the report states the background and the basis of the work that was made. Then, in chapter 4, follows a description about how the work behind the concept development was carried out. Chapter 5 presents the research and existing concepts which will help in developing a new concept, this can be considered part of the result of the method used in chapter 4. Then in chapter 6 follows a description about how the selected concept where to be refined in terms of level of detail and strength calculations made on the selected concept. In chapter 7 the result of the research is presented as a selected concept. The results of the work to refine the selected concept is also presented here as well as the concept in its final form. Lastly in chapter 8 is a discussion about the work carried out, followed by conclusions and recommendations for future work.

4 Method for concept development

This chapter describes how the project was performed. Figure 4.1 shows a flowchart which describes the workflow throughout the project. This chapter describes the method used in the first part of the thesis, the concept development.

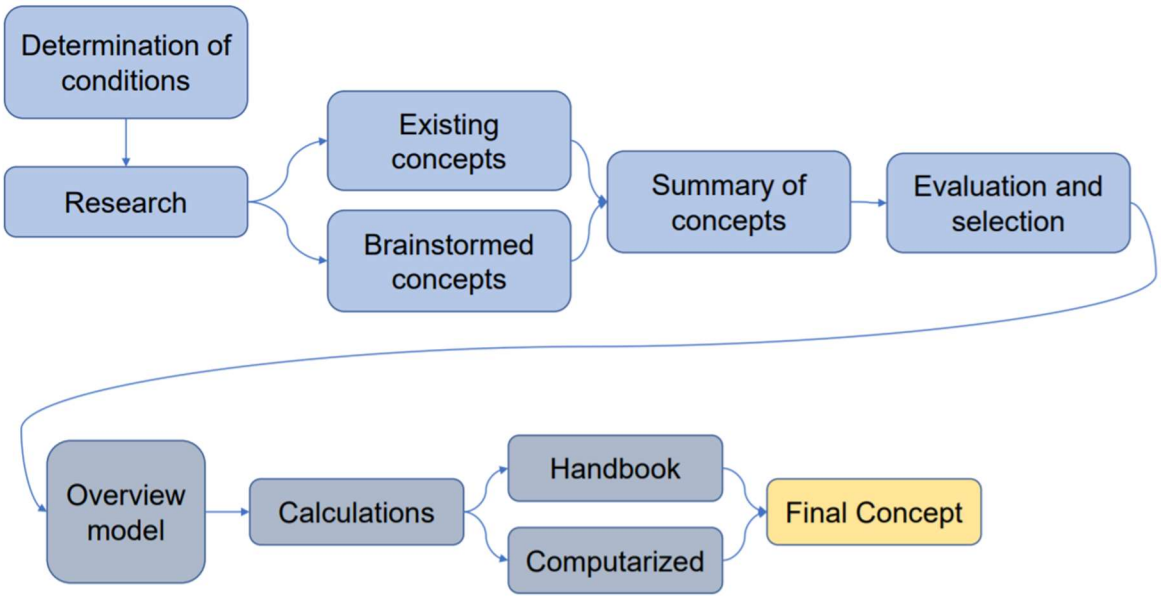

Figure 4.1 Flowchart of the workflow during the concept development, starting at the top right.

4.1 Determining conditions

To ensure that the concept developed suits the task and meets the conditions, requirements and criteria set by this task an analysis of the conditions is required. One important condition is the fact that the system is to be used in saltwater. Other conditions include the platform's measures, forces involved and requirements from the sailors. To find these, consultations was made with Formula Sailing and its members. As well as consulting experienced Moth sailors for their input on the control of the system.

Some conditions will directly impact the concept, measures for example, and will be considered criteria. While others, like how the system should be controlled, can be considered desires. These criteria has already been presented in chapter 2.

4.2 Research on existing concepts and brainstorming

To find out what concepts can meet the criteria, research on the existing concepts on the market was carried out. This included looking at information at events such as "Foiling week" (Foiling Week, 2020) where most of Europe's foiling sailboats gather to share experience, consulting Moth sailors and browsing the internet. Not a lot of academic publications have been released on foiling for sailing crafts. Most innovation is made privately and kept within the companies. There are research and developed concept on foiling control systems motorized crafts, but that

research is not relevant since no forces provided from other sources then the wind and crew is allowed. However, a summary of past work carried out by Chalmers on the topic was included.

Adding to this was a series of brainstorming occasions with Formula Sailing to find out what ideas where previously thought of by its members. This information could then be used as inspiration for this project and for future work. The research gathered in these steps are presented in the following chapter.

4.3 Summary and evaluation of concepts

The concepts that turned out in the research could then be summarized and evaluated regarding the design criteria. This includes ranking of concepts by the Pugh-method and consulting experienced sailors. Different concepts of the entire system could be made in sketches. The different concepts were then introduced to Formula Sailing for further evaluation until a final concept path could be decided.

A simple overview picture could now be formed and the base dimensions to its parts could be decided. The future work of refining the concept could then proceed, this is presented in chapter 6 and 7.

5 Currently used systems and solutions

In this chapter previously used systems and solutions will be presented and investigated. Solutions from other mechanical areas that might be of interest will also be investigated and presented here. Note that no variables from this chapter will be listed, unless the solution is brought to the final concept. Friction has been noted but not considered in the calculations for solutions in this chapter.

5.1 Full systems

A system with two individual flaps on the same wing has to our knowledge never been used, therefore it is not possible to base this design on an existing system but gather inspiration and knowledge from systems used in other classes.

The international Moth class with its big fleet and a broad variety of designers is currently leading development in foiling for dinghies. To investigate what kind of control systems have been used with success is where to start. The McDougall built Mach 2 is the most common model of Moth in the fleet (Mach2boats, 2019). The Mach 2 control system acts in the same way as shown in figure 2.4.Figure 5.1 shows a simple drawing of the Mach 2 control system.

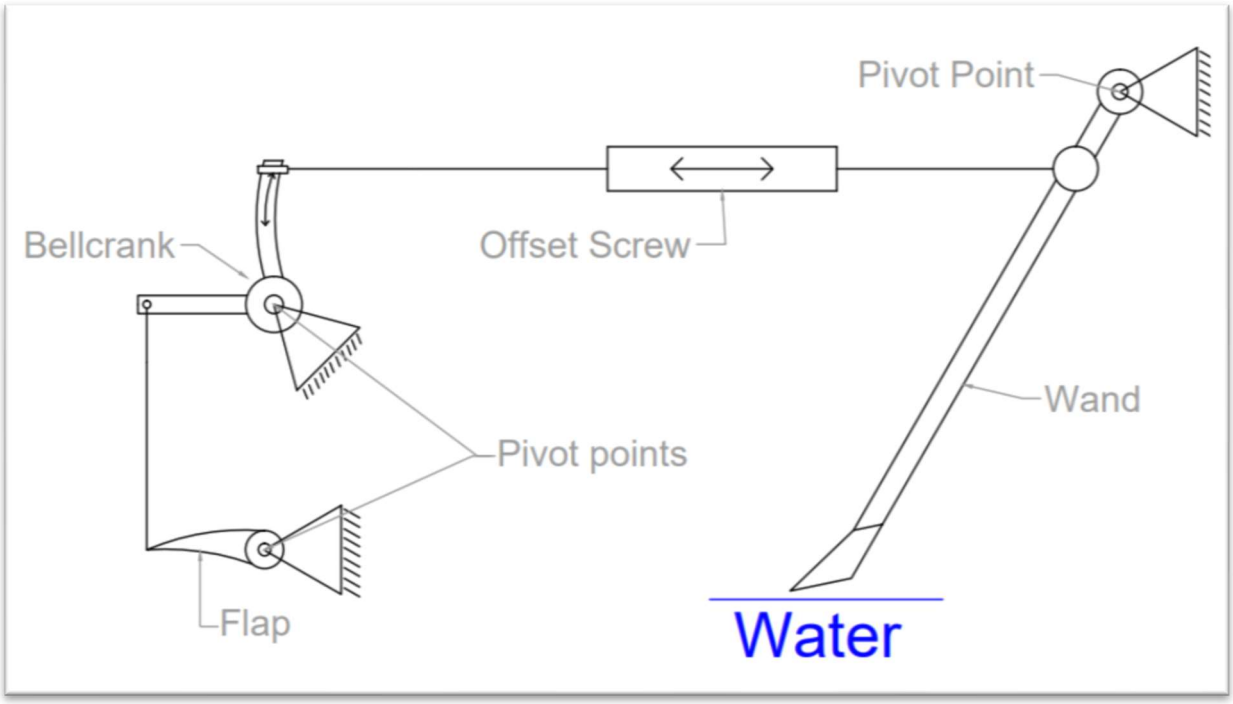

Figure 5.1 Simple sketch of the function of the Mach 2 control system (not to scale)

This system consists of a height measurer called “wand”, that skims the water surface and gives an angle input to the system depending on the ride height of the boat. The wand is telescopic and can, therefore, change the given angle at a given ride height. This controls the gain of the system and it also changes its behaviour in waves. Through a wand pivot this angle change gives a pushing force on a control wire or rod. On some configurations, this is transferred to a pulling force through a gear. On this rod an offset screw is mounted. This tube is connected to one rod on each end through opposite threads, Rotating this tube will increase or decrease the length of the rod, offsetting the signal from the wand. Next the rod is connected to the bell

crank which is a slightly bent pivoting rod. The height of this connection can be adjusted and thereby making the system more or less responsive. This is the main gain control of the system. The signal is then transferred to the main foil pushrod which connects to the flap of the foil. This is a simple and well-tested system that gives the sailor a lot of manoeuvrability and options in flight control.
Other active Control systems have been inspired by the Moth class and are therefore very similar. One of these is iFly15's Flysafe® control system (iflysail, 2019), where it is stated that the system is "based on the iMoth". The system sits on a catamaran and has two separate T-foils which makes it similar to Linnea's new design. Exactly how the system works is unknown, but it is stated that it is controlled by one rope, controlling the preferred foil angle and ride height. The wands have fixed length and on the pictures on the website, you find that a length-dependent purchase system is used, similar to the gain system on the Moth. The system uses "differential ailerons" (iflysail, 2019), in other words, the flaps have a lower purchase when going to negative flap angles. The reason for this is hydrodynamical and outside of this thesis area, but a dynamic purchase/gain system will give more options in controlling the foils. There is no evidence that the starboard and port system is connected in any way.

5.2 Partial solutions

Looking into the control systems used today and bearing in mind the complexity and demands put on Linnea's control system it will not be possible to copy one of these systems but use them as inspiration. To further investigate design options, different functions will be researched separately, these functions will be divided into five categories bearing in mind the demands set by the flight dynamics specified by Formula Sailing. High reliability and accuracy will be the overall aim.

- Height and heel measuring

Measuring the ride height of Linnea accurately will be crucial. All the force needed to deflect the flaps will be provided by the height measurer.

- Linkage and connection

The signal will have to change direction at least once before going into the foil. There are lots of ways to change the direction of a mechanical signal. Connections between a wand, flaps and the control system can also be done in several ways.

- Signal offset

Similar to the function of the offset screw on the Moth, Linnea will have different preferred flap angles at different wind speeds and conditions (Prabahar, 2020). Also, to utilize the performance mode the flaps will need to have the possibility to be offset from tack to tack. This calls for a quick and powerful offset system as well as a fine-tuning one (Boman, 2019).

- Gain adjustment

The gain has been set by Formula Sailing to match a specific wind speed. If the wind speed changes, the gain needs to be changed as well (Prabahar, 2020). However, it can be done in between races and does not have to be a fast solution.

- User controls

The sailors should have to make as few adjustments as possible enabling them to focus on sailing. But when needed the sailors need to have the opportunity to adjust the control system

to trim the boat properly. The system needs to be user friendly and intuitive to make the learning curve steeper in training.

5.2.1 Height and heel measuring

The height of the vessel is the input signal to the control system. This measurement must be accurate and continuous. A way to measure the heel of the vessel must also be investigated to meet the foiling criteria. This chapter will investigate these topics.

5.2.1.a The classic wand system

Figure 5.2 The Mach2 wand solution (Boman, 2019).

The wand system is the most used system and its simple design gives it a lot of robustness and reliability. It consists of a rod that is pivoting around a fixed point on the boat (1) in figure 5.2. On the other end of the rod there is a shovel-like part which is designed to plane on the water surface with as little drag as possible (2). The rod itself (3) is telescopic and spring-loaded with a rope attached, so that the sailor can adjust its length. The signal given by the wand depending on ride height is in the first instance an angle, but another rod is connected to the wand transferring the signal to a pulling/pushing force depending on if the connection is above or under the wand's pivoting point. The output position of the first connecting rod horizontally (L_c) depending on the ride height (H) can be described by equation 7. The variables are displayed in Figure 5.3.

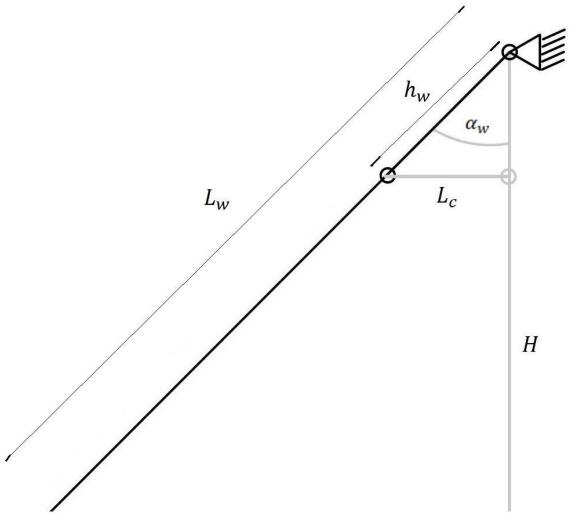

Figure 5.3 The schematics of the Mach2 wand system

$$H = L_w * \cos(\alpha_w) \quad \textbf{(7)}$$

And

$$L_c = h_w * \sin(\alpha_w) \quad \textbf{(8)}$$

Insert 7 in 8

$$L_c = h_w * \sqrt{1 - (\frac{H}{L_w})^2} \quad \textbf{(9)}$$

This shows that the change in position of the connecting rod is linked non-linearly to the ride height with a leverage factor between the wand's length and the connecting rod's distance from the pivoting rod. L_c and h_w are specific to this system and not considered variables. With the relation between wand and rod being non-linear it gives a larger output signal per change in ride height when the boat is close to its maximum ride height and a lower output when the boat is low in the water. This could provide issues further down the system if it must be compensated for. The force input on the wand comes from the shovel-like part on its end and will always be perpendicular to the wand. The forces acting on the wand are shown in figure 5.4

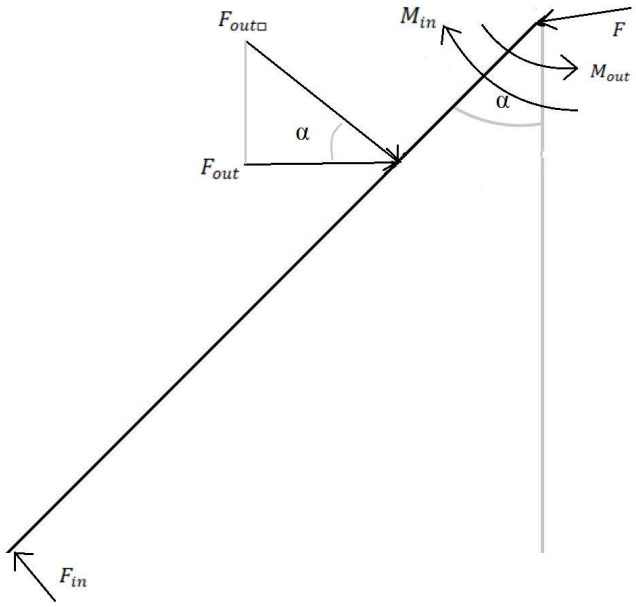

Figure 5.4 Forces working on the wand

Here the output force from the flap is almost always connected to the wand with an angle, which means that the force providing torque to the wand is dependent on this angle, described by $F_{out□}$ in equation 10.

$$F_{out□} = \frac{F_{out}}{\cos(\alpha)} \quad \textbf{(10)}$$

Since $\cos(\alpha)$ is always smaller than or equal to 1 $F_{out□}$ will always be bigger or equal to F_{out}. The torque as a result of this force is described by equation 11.

$$M_{out} = F_{out□} * h_w \quad \textbf{(11)}$$

And the input torque.

$$M_{in} = F_{in} * L_w \quad \textbf{(12)}$$

For equilibrium equation 13 must be true.

$$M_{in} = M_{out} \quad \textbf{(13)}$$

Inserting 10 and 11 into 12 and solving for F_{in}

$$F_{in} = \frac{\frac{F_{out}}{\cos(\alpha)} * h_w}{L_w} \quad \textbf{(14)}$$

Therefore, the input force is dependent on the output force described in equation 14. To optimize this design by reducing the input force the wand would have to be as long as possible and the distance from the pivot where the connecting rod meets the wand has to be kept small.

5.2.1.b Articulated wand

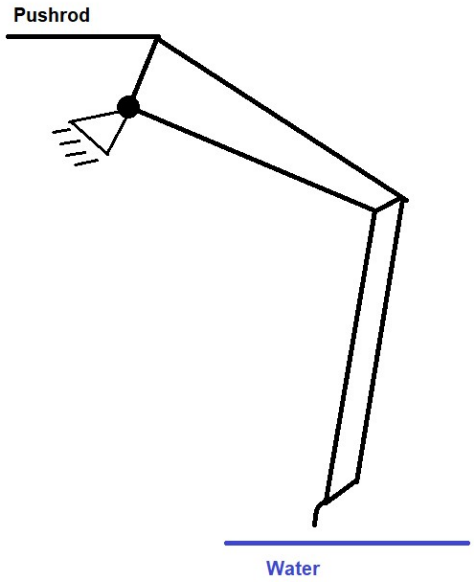

Figure 5.5 Side view sketch of a articulated wand (hartasproductions, 2020)

On some occasions, Moth sailors have been seen sailing with an articulated wand shown in figure 5.5 (hartasproductions, 2020). This design works in the same way as a classic wand but it allows for the measurement of height to be taken further forward relative to the boat. In theory this should provide better performance in waves since the boat will have more time to react to the movement of the flap before the wave reaches the foil. However, if the wand is extended forward of the boat it will extend the overall boat length and might break the box rule of which the boat was built to fit in.

5.2.1.c Measuring heel

Measuring heel will be a crucial part of making the individual flap system work. But to use an individual sensor for measuring heel mechanically would be almost impossible. The best mechanical solution would be a pendulum which would also measure the acceleration of roll. (FormulaSailing, 2019). Although, to generate any force from such a system would require it to be big in size and therefore heavy and not suitable for this task.

However, the initial idea to use two height sensors can give an output in heel as well. By measuring the difference in the output of the two height sensors the heel can be measured. (FormulaSailing, 2019) Figure 5.6 shows how a – b = heel.

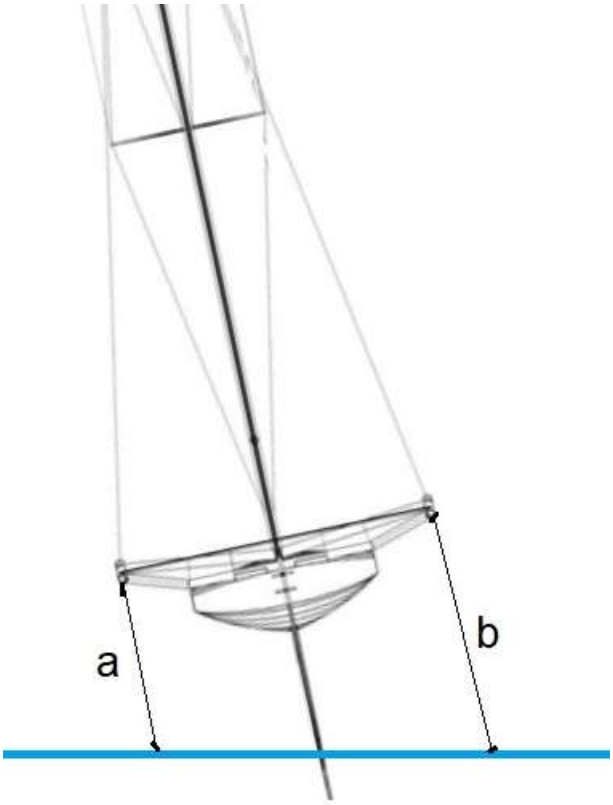

Figure 5.6 Heel measured with height sensors

There is a difference between actively or passively using the difference in the output signal from the height sensors. By using a passive control there will be no actual measurement of this factor but the difference is transferred to the flaps without any modification depending on the heel. However, a pre-programmed change can be added, for instance, a height dependent gain change for each flap would passively act like a heel dependent system. But for hydrodynamic reasons, Linnea might at some point benefit from having a third input that modifies the signal to the flap. An example would be that the gain of the movement should be greater to the side that she heels too. Then the gain would have to be changed depending on the difference in output from the height sensors thus there will have to be a third sensor which indicates heel.

One way to do this is to have the two signal rods or extensions of them, push on a pivoting beam or rod, the angle of this rod would then be the output for the heel (FormulaSailing, 2019). To allow any non-linear changes in each signal rod, like waves, there would have to be some flex in the pivoting rod not to put extra stress on the whole system. Figure 5.7 shows a sketch of this solution.

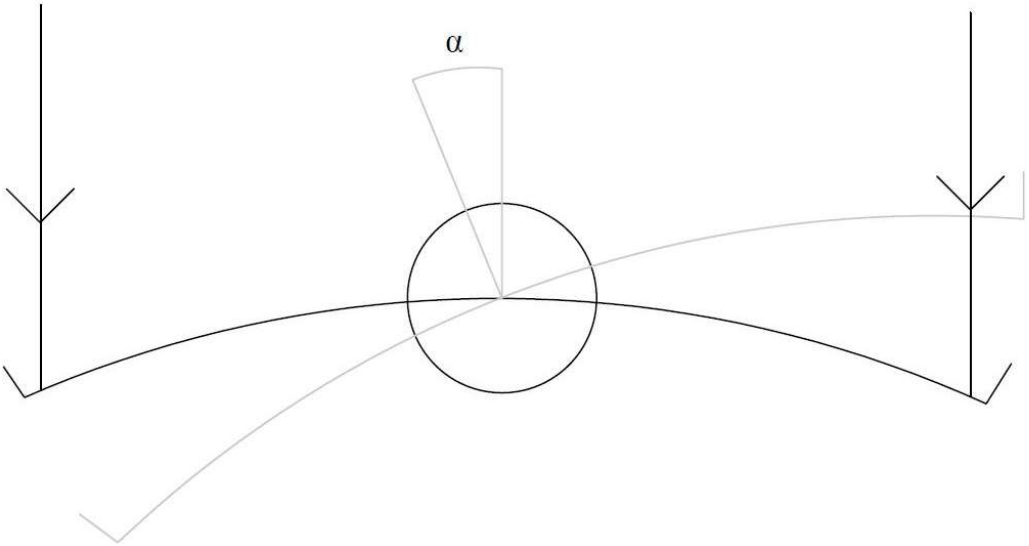

Figure 5.7 Sketch of heel measuring system with the output α.

A system like this would have a dampening effect on the heel to make sure only the actual heel is measured and no interference from waves etc. The material demands on the pivoting rod would be high and require a lot of thought not to be too stiff at the same not too weak. The rotation of the pivoting rod can easily be transferred into any change in signal. However, this system would not be linear from the start, but different shapes and gearing can adjust that issue (FormulaSailing, 2019).

5.2.2 Linkage and connections

5.2.2.a Linkage

So far only rods have been considered to transfer the signal through the boat. This is because it is the most used solution in foiling dinghies, however, there have been attempts to use other methods. In the Dackhammar (Dackhammar et al, 2018), wires were considered to transfer the signal from sensors to the flaps. The argument to why Dackhammar, et al chose wires is unclear, and based on Formula Sailing's calculations the system will on some occasions experience negative forces. This would make the use of wires impossible since they cannot handle pushing forces and therefore change in direction of forces will not be applied.

Rods also have their limitations especially under high load, then a rod can buckle and store energy which might be released later when the pressure drops, creating an uncontrolled increase in lift, or the rod might break (Boman, 2019). To avoid any unexpected changes in the system caused by the rods they will have to be dimensioned precisely to save weight and supported in ways that make sure no bend occurs in the rods.

At some point the motion in the system might have to change direction, to do this with wires is easy since they are flexible, but changing direction of a rod is harder. The easiest way to do it is to have the rods connect to a L-shape part that pivots around its corner the motion can then be angled (FormulaSailing, 2019). Figure 5.8 shows this part and the connecting rods.

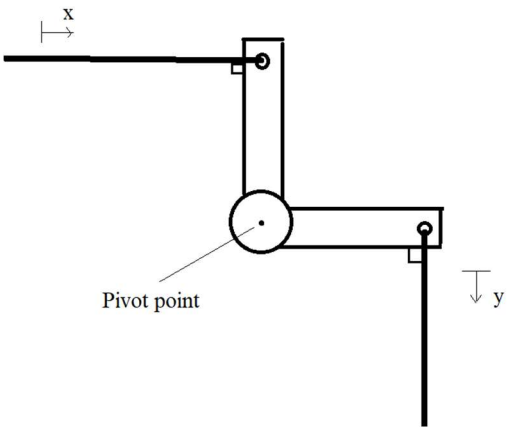

Figure 5.8 Pivot-point for push/pull system

In this way the distance change in x-direction for the rod attached from the left will be the same distance travelled in y-direction by the rod going down. If the pivot arms have different length this could also be used to change the gain of the signal. Also, if the pivot arm to the right of the pivot point is positioned to the left of pivot point instead, the system would change direction. A pushing signal in x-direction will then be pulling from y. As long as the base angle between the rod and the arm is square on each side of the pivot at the base pivot angle the signal will be transferred without interference from trigonometric aspects of the pivot, even if the angle between the arms is changed.

As a third option to link the two ends of the control system hydraulics can be used (FormulaSailing, 2019). In bigger applications such as superyachts and the Americas Cup, hydraulics are being used to control foils. The possibility to transfer motion from one point to another with only a hydraulic tube would be an appropriate solution for this application as well.

5.2.2.b Flap connectors

The way the control system connects to the flap is what all designs should start. How this connection is made characterizes the whole system. The distance from where the flap pivots to where the system connects changes the load put on the system, a larger distance will provide less load. The iFly Catamaran solved this issue by moving the centreboard aft on the foil allowing the connection to be as far aft as possible, it even has an extra platform on the flap for the connector to sit on, see figure 5.9 (CEC Catamarans, 2019).

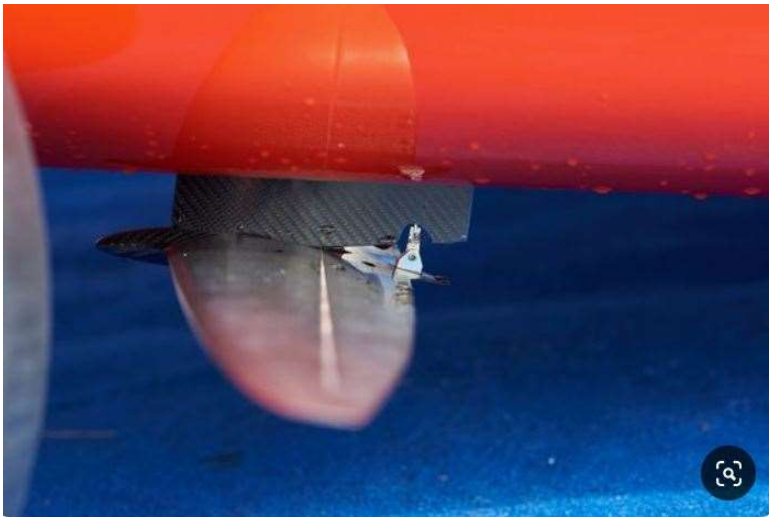

Figure 5.9 iFly catamaran foil connector (CEC Catamarans, 2019)

On the Mach2 a rod connects the two sides of the flap and goes into the actual flap. The control system connects to this rod. This allows the force to be distributed in a larger part of the flap, reducing twist throughout the flap, see figure 5.10.

Figure 5.10 Mach2 foil connection (Boman, 2019).

In our case, two control rods will come down the centreboard to connect to the two flaps. The solution previously suggested by formula sailing (Dackhammar et al, 2018) due to the lack of space in the centreboard was to have the rods come down in front of each other. The flaps then connected at the same distance from the flap pivot. However, the dimensions of the foil and centreboard have changed since then, and there is no way for the connectors to pivot themselves. This solution is shown in figure 5.11.

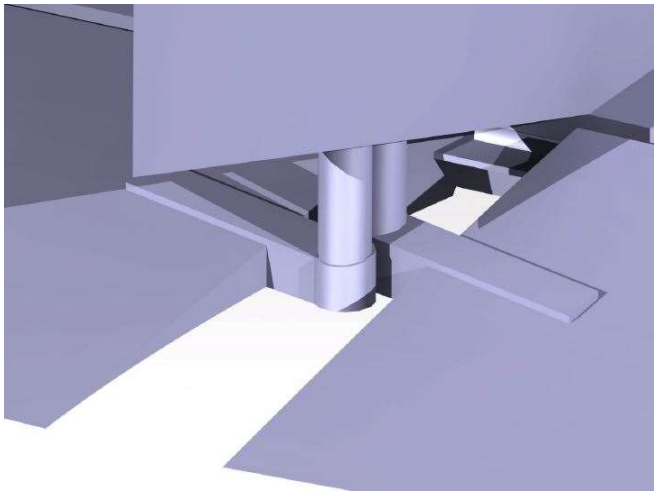

Figure 5.11 Connectors developed by Formula Sailing (Dackhammar et al, 2018)

The connectors should be fitted as far back on the flap as possible and distribute the force over the flap to avoid any stress-related issues in the design. If more space was available a lot of different solutions could be implemented. For instance, there can be several advantages to have spinning control rods instead of having them move laterally. The connector solution would then require a worm gear. However, this would require a lot of gears through the system which is not working well in salty conditions.

Another option to connect the system to the flap is to invert the motion to a pulling motion by extending a lever in front of the flap pivot (FormulaSailing, 2019). The advantage of having a pulling rod instead of one that pushes is that the risk of buckling the rod is eliminated. That would allow for a thinner rod saving weight and space. However, this option will require space inside the actual foil which might be a hydrodynamic disadvantage. This does not have to be all negative though, since the pull rods can then be positioned where the centreboard is wider, which allows for even more space and freedom in design. If the vertical and horizontal part of the foil cannot be separated this would be very hard to assemble.

In this design the flap angle, α_f can then be described with the lever L_f and the distance the rod has travelled to achieve this angle, shown in equation 15. The variables are shown in figure 5.12.

$$\alpha_f = sin^{-1}(\frac{x}{L_f}) \qquad \textbf{(15)}$$

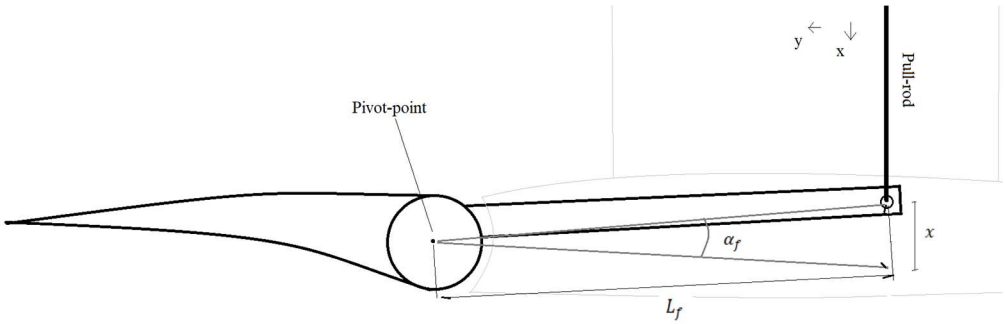

Figure 5.12 Flap-lever geometry

5.2.3 Signal offset

To be able to offset the signal from the sensor to the flaps will be crucial. In different conditions different offsets will be needed to control flight. To be able to use the extra leverage potential of the system discussed in chapter 2.2 an offset will have to be made to each side. This can be done in several ways., Presented below are the ones used in sailing and other ways of lengthening or shortening a rod. As little input force as possible should be used since it needs to be produced by the boat itself. Therefore, spring-loaded release systems will not be considered since the force needed to release the lock will be bigger than the force the lock needs to hold. If the system would only experience forces in one direction a rachet system could be used but that is not the case.

5.2.3a The Mach2 offset screw

Figure 5.13 (1) shows a picture of the Mach2 offset screw. It consists of an outer tube which has two nuts on either end. These nuts threads have different directions and can therefore increase or decrease the length of the connecting rod.

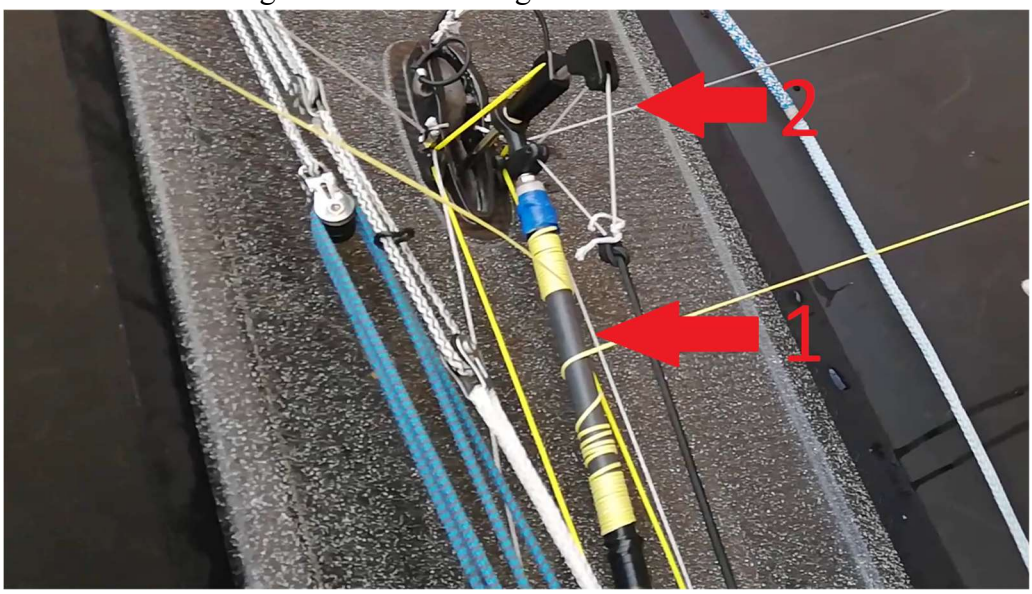

Figur 5.13 Control System of the Mach2 (Boman, 2019).

Figure 5.14 shows a section of this design. The outer tube is rotated by pulling a rope that is coiled around the tube, increasing or decreasing the offset.

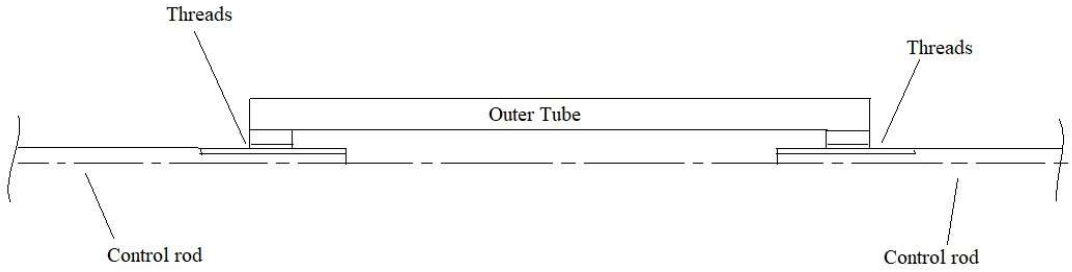

Figur 5.14 Section of the Mach2 offset screw (Boman, 2019)

5.2.4.b Telescopic rods

To change the length of a telescopic rod can be achieved in many ways, the simplest one is the friction-based one where a lever can be pulled or a bushing screwed to decrease the radius of the outer tube. Much like a telescopic broomstick. Figure 5.15 shows this mechanism. Also, to the right in figure 5.15 there is the briefcase solution where spring-loaded pins click into grooves or holes in the outer rod, quickly and automatically locking the rod length. All these solutions need two input-forces to work, one that locks/unlocks and one that adjusts. Also, the briefcase solution requires hollow rods which decreases its strength.

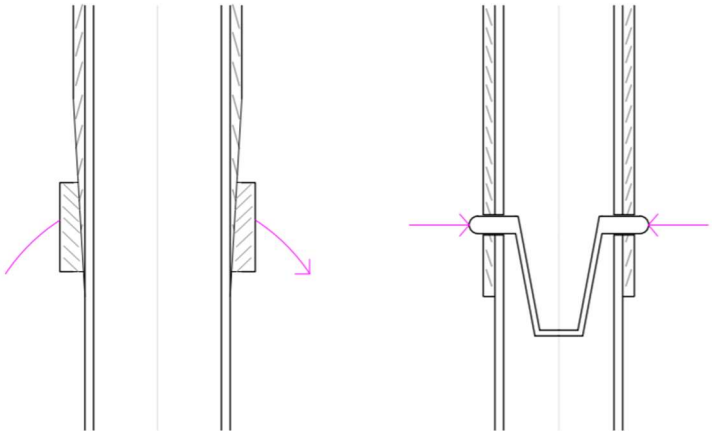

Figure 5.15 Different solutions of telescopic locking mechanism (Boman, 2019)

5.2.4.c Pivot-point offset

Looking at chapter 4.2.2.a a pivot-point can be set at different position to change the offset of the signal. If the pivot-point is moved in one of the rod directions the signal would be offset with the same distance as the pivot-point is moved (FormulaSailing, 2019). Changing the position of fixed points on the boat would be easier than changing the length of the rods since the rods will be moving while sailing. To make this change a ball lock system would be appropriate to lock the shaft of the pivot in preselected positions to fit the flight dynamics. Moving a pivot would change the angle of one of the rods going into the pivot, however, for long rods this can be neglected for small offsets.

5.2.4 Gain adjustment

5.2.4.a The Mach2 system

The purchase system on the Mach2 is a lever length-based system and is shown in figure 5.13(2). By changing the position of the connecting rod on the bellcrank a different gain can be achieved. This is manually done by the sailor (Boman, 2019). In figure 5.13 it is shown that the bellcrank is slightly bent, this is to make the connecting point follow the arc of the connecting rod from its pivoting point. This enables the system to not have a different offset due to different gain. A sketch of the bellcrank is shown in figure 5.16, and the equation describing the gain factor is simply the distance from the pivoting point of the centreboard push rod divided by the distance between the pivoting point and the connecting rod connection.

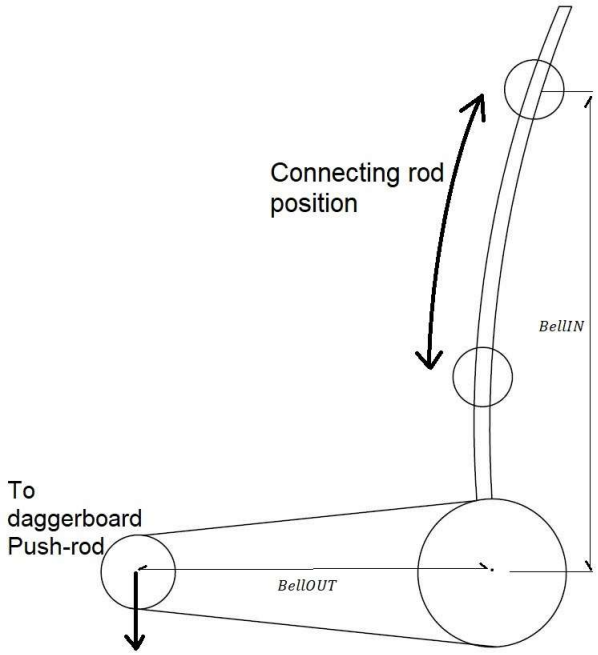

Figure 5.16 Sketch of the Mach 2 gain system schematics (Boman, 2019)

The force needed to move the connecting rod position is only determined by friction. And the gain factor G is determined by the lever arms ratio in equation 16. For force calculation the opposite purchase is used. What you gain in speed you lose in power.

$$G = \frac{BellOUT}{BellIN} \qquad \textbf{(16)}$$

5.2.4b The BugsCam

Created in 2016 by Phill 'Bugs' Smith, the BugsCam is designed for the Moth and features a wand just like the Mach2 but instead of directly connecting to the control rod the wand is connected to a metal plate called the 'cam' ('Bugs' Smith, 2019). The connecting rod is fixed in all dimensions but one, only enabling movement in one direction. On the end of the connecting rod is a wheel that rides the curve of the cam, producing a signal depending on the position of the wheel horizontally. This gives the designer a lot of opportunities in designing flight dynamics. A schematic sketch is shown in figure 5.17

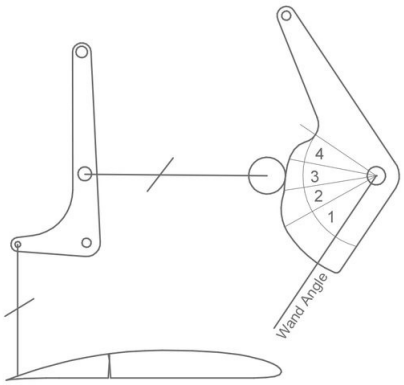

Figure 5.17 Sketch of BugsCam ('Bugs' Smith, 2019)

In this design, the bellcrank has a 1:1 ratio meaning that the actual distance the wheel travels is the distance the centreboard
push-rod travels and therefore this system removes any complicated trigonometry involved in the traditional push system. The non-linear behavior of the wand can also be removed by shaping the cam. Smith aimed to design a cam which made the boat go up to ride height faster, stay at ride height longer and safely dropping down if the boat got to high. The result is visible in figure 5.18, with big wand angles when the boat is low in the water the wheel is at a long distance from the center of the pivot in zone 1, providing maximum lift. As the boat starts to lift wand angle is reduced and the wheel is quickly moved into cone 2-3. If the boat would fly too high the wheel would enter zone 4 where the distance is rapidly reduced quickly reducing lift making it impossible for the boat to jump out of the water.

This system also decreases the force put on the wand since the wheel is pushing in a straight line between the bellcrank and the cam pivot. Most of the force needed to keep the flap in place is then taken up by the cam fitting. Figure 5.18 shows a detailed sketch of this.

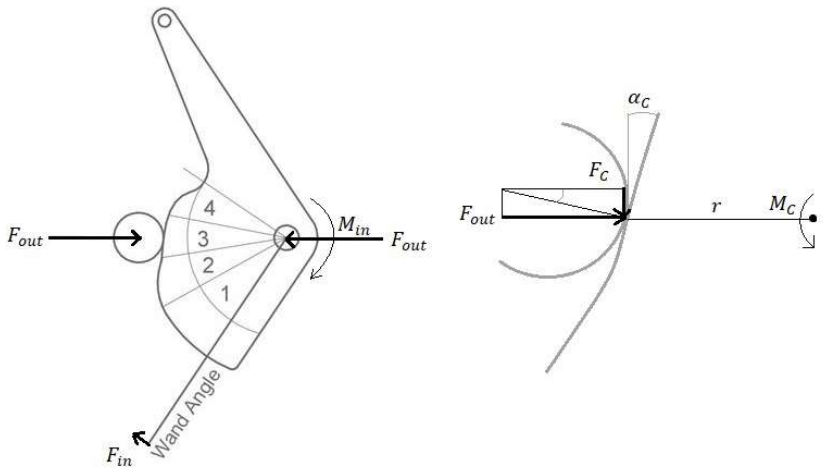

Figure 5.18 Forces acting on the cam ('Bugs' Smith, 2019)

Looking at the gemometry in figure 2.4 the torque at the wand is described by equation 17.

$$M_{in} = F_{in} * L_w \quad \textbf{(17)}$$

In this case F_{out} is cancelled out at the cam fitting leaving F_C as a function of the slope of the cam. The slope is described by α_C. F_C is then described by equation 18

$$F_C = F_{out} * \tan(\alpha_C) \quad \textbf{(18)}$$

Further the torques acting on the cam are given by

$$M_C = F_C * r \quad \textbf{(19)}$$

And since there are no further forces acting on the wand, equilibrium is described by equation 22.

$$M_{in} = M_C \quad \textbf{(20)}$$

Inserting 18 and 19 in 20 and solving for F_{in}.

$$F_{in} = \frac{F_{out} * \tan(\alpha_C) * r}{L_w} \quad \textbf{(21)}$$

For small slope angles, this design removes a big part of the force needed to keep the flap in place from the forces acting on the wand. Instead, a large portion of the force is taken up by the cam fitting. The input force needed can thereby be greatly reduced which will decrease hydrodynamic drag significantly. To optimize this, the slope should be as low as possible to make the $\tan(\alpha_C)$ coefficient small. But at the same time decrease the lever that F_C has by decreasing r.

5.2.3 User controls

To meet the criteria of easy handling the system should act without sailor interference to the largest extent to make it easy to handle (Boman, 2019). The sailors should be able to use the boat as tan extension of their arm without thinking about changing settings or adjusting screws. But if the sailor needs to make a change to the flight dynamics during a race it has to be easy to make this change. An easy way to control the system for the sailors would be to use ropes. Ropes have the benefit of being light, flexible and strong, although ropes have their limitations when it comes to precision. They are seldomly 100% rigid and usually, a rope is locked in a jaw, cleat or with a knot where there is always a potential slip. Even if there is a pre-set length to the adjustment over time you cannot be sure if the rope will stretch or shrink. Control by a lever or wheel that connects to a rod is an alternative to increase precision if needed. For controls that can be changed in between races, a slower but more simple system can be used. The controls of the system can therefore be divided into slow and fast controls.

6 Method for concept refinement

Figure 4.1 shows the next step of the method used, calculations and final concept. When a concept was decided based upon the information gathered in chapter 5 calculations on the system could be carried out to develop a more refined and easy implemented system. First the flight dynamic performance was evaluated to meet Formula Sailing's criteria. Important features requested by experienced foil-sailors were also taken into consideration when the flight dynamics was calculated.

Secondly calculations on the system's strength was carried out. Many of the parts could be dimensioned for the forces estimated with handbook formulas on structural integrity by Tore Dahlberg (Dahlberg, 2001). Such as resistance to buckling, shear forces and beam bending. While more complicated parts were evaluated for strength with a FEM program in the computer aided design program CATIA. These parts where modelled and and simulated to mimic the real forces put on the parts to make an in-detail analysis of the parts strength.

6.1 Final concept

With all the parts dimensioned and calculated, a model of the final concept could be built, this was carried out in a CAD program to easily be implemented in Formula Sailing's model. This allows for easier future work with each part visualized. Also, the system is easily implemented, since the models can be made into production drawings.

7 Result

This chapter consists of three parts. Concept selection, which presents the result of the research made in chapter 5. Derivations, which presents the necessary math behind the final concept and what this results in in terms of numbers. Lastly, final concept and models, which presents the visual and mechanical aspects of the concept.

7.1 Concept selection

Table 3 shows the Pugh matrix used to decide on the different parts of the concept.

Table 3 Pugh matrix of the concepts of the different sub systems. To the left is the different aspects of the sub system and at the top the different solutions are listed. A total score is given to see how the solutions compare to each other. The Moth system was set as a benchmark to compare with.

Selection Matrix	Value	ALTERNATIVES																				
Citeria		Height and Heel	Classic Wand	Articulated	Passive Heel	Active Heel	Linkagae	Rods	Wires	Hydraulics	Flap connection	Mach 2	iFLY	Formula sail	Pull lever	Signal offset	Mach2 Screw	Telecopic rods	Pivotpoint offset	Gain Adjustment	Mach 2	Bugs Cam	User controls	Ropes	Levers	Screws
Performance																										
Accuracy	3		0	0	-1	1		0	-1	0		0	0	0	1		0	0	0		0	1		0	1	1
User experience	1		0	1	1	0		0	-1	0		0	0	0	0		0	-1	1		0	1		0	1	-1
Adjustability	3		0	-1	0	0		0	0	0		0	0	0	0		0	-1	-1		0	1		0	0	1
Speed	2		0	0	0	0		0	0	0		0	0	0	0		0	1	1		0	1		0	1	-1
Weight	1		0	-1	0	0		0	1	1		0	1	1	-1		0	-1	1		0	-1		0	-1	0
Simplicity																										
Number of parts	1		0	-1	1	-1		0	0	1		0	0	-1	0		0	-1	0		0	-1		0	0	0
Manufacture Simplicity	1		0	-1	1	-1		0	0	-1		0	-1	-1	0		0	0	0		0	-1		0	-1	-1
Assembly Simplicity	1		0	-1	1	-1		0	0	1		0	-1	-1	0		0	-1	0		0	0		0	0	0
Robustness																										
Managing forces	1		0	0	0	-1		0	-1	1		0	1	0	1		0	-1	0		0	1		0	1	1
Weak spots	1		0	-1	0	-1		0	0	1		0	1	0	1		0	-1	0		0	1		0	1	1
Risk of failure	2		0	-1	0	-1		0	-1	0		0	1	0	1		0	-1	-1		0	0		0	1	1
Total			0	-9	1	-4		0	-6	4		0	3	-2	6		0	-9	-1		0	8		0	8	6

The selection of the final concept was made together with the Formula Sailing team to make sure that the system meets their requirements. The system selected will feature

- A traditional wand

The wand solution is a well proven concept and have a lot of advantages built into the design, the accuracy and speed in relation to the relatively low drag makes it a natural choice.

- Passive heel measuring

The complexity sets the restrictions in this area. It would be an advantage to have a flight design which responded to the heel as a variable. However, that would require a system with a lot more complexity. Formula Sailing considered a passive system to still be a great improvement in-flight stability and the passive option was selected.

- Connecting rods with pivot-points

To assure precision in the system rods was selected, the rods must be of stainless steel. A precise calculation must be made on the rods resistance to buckling to save non-renewable weight. Tale 5.1 shows that hydraulics would be better than rods, but at this time no parts that would fit the task was found.

- Flap connection

To enable more freedom in future work on structural strength of the foil, the pull-system connection will be applied to the design. It allows a smaller vertical part of the foil and it allows it to be positioned further forward on the horizontal foil. Also, it eliminates almost all possibilities of buckling the control rod, enabling a thinner rod in the centreboard saving weight and enabling even more freedom of where to position the rods. However, the final signal must be transferred to a pulling signal before entering the foil. Due to the potential hydrodynamic advantages and the standout result in Table 3 this selection is a great option to improve the design.

- Signal offset in Mach2 offset screw and a manual pivot-point offset option.

Here the well tested Mach2 screw shows to be the best option and should therefore be the pre-set offset control that would be tuned in between races to match the condition. But compared to the pivot-point offset solution an offset screw is slow but enables more freedom in the adjustments. The system will therefore feature both solutions, the offset screw will be complemented by a pivot point offset system that can be changed quickly while sailing, also enabling the performance mode.

- Interchangeable Cam gain system with alternative gain adjustment

Here a compromise between the two options was chosen. The advantages of the cam system are obvious, it allows precise control of the flight and it enables some interesting flight design with removal of the non-linearity of the wand. The cam will be interchangeable to adjust for different conditions. A way to handle the negative forces needs be considered as well. If conditions that do not fit the cam are encountered a way to adjust gain manually is needed. This will be done by changing the purchase of a bellcrank, similar to the Mach 2 gain control.

- Mechanical user controls

Changes to the system by the sailors will be made in different ways. Setting up the system before sailing will be done by turning nuts and screws to change the base offsets and gains. While sailing, only one control is at the hands of the sailors, the performance mode enabled by the pivot offset. To change the pivot offset a lever can be pulled manually or extended via a rope from the racks for easy access while sailing.

The parts will be made mainly from stainless steel with the characteristics described in Table 2. To have parts that will not stain in salt water is crucial in this design. Therefore this material is selected. At some points plastic may be used to allow easier replacement or decrease wear on structural metal parts.

Figure 7.1 shows an overview drawing of the control system implemented on Linnea. Black lines represent new parts involved in the control system. The first important change is that the racks should be extended as far forward as possibly allowed to increase the systems responsiveness to waves (Boman, 2019).

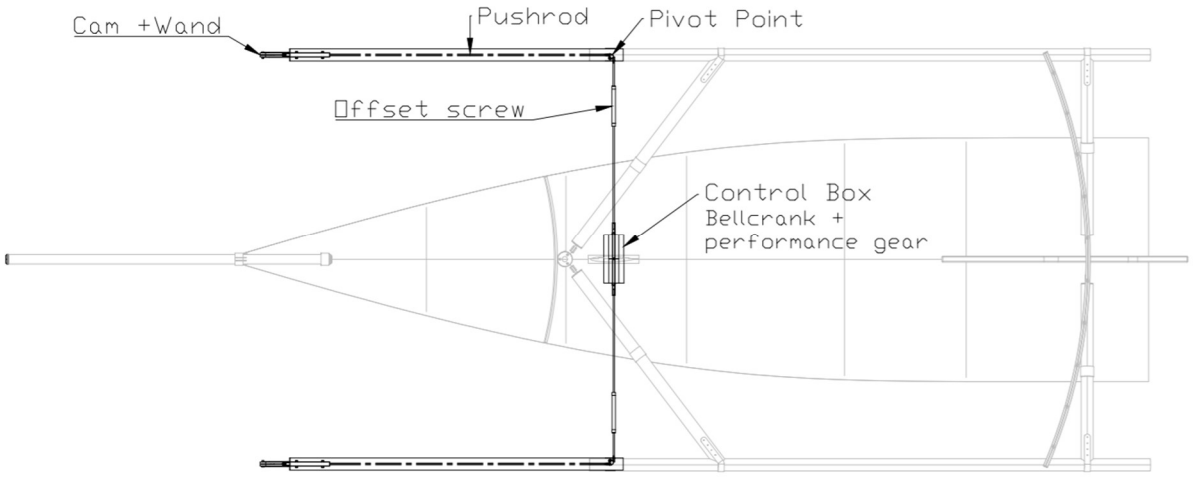

Figure 7.1 Overview of the control system, black lines represent the new parts related to the control system.

7.2 Derivations and Calculations

This chapter presents the result of derivations and calculations made on each part in the system needed to achieve a more detailed result. It may be considered part of the method used but the purpose of this chapter is to understand what variables are taken in consideration and what aspects of each part is important for future work on the system. If not otherwise stated the factor of safety is 1.2.

7.2.1 The wand

The wand is the input of the system, starting the calculations here will make the rest of the work easier. To start with, equation 1 is measuring height from the waterline, whereas in this project height will be measured from the racks where the wands are connected. The 3D models of Linnea were measured, and a new definition of H was decided.

$$H_2 = H + 417\ mm \qquad \textbf{(22)}$$

H_2 is described by the angle of the wand. Looking at equation 9 in chapter 4 the height is described as a cosine function of the ride height and the wand length, the wand length must be decided. To do this the geometry of the boat was examined, and a preferred ride height angle of 40 degrees was decided. With the preferred ride height of $H(rideheight) = 65cm$ gives $H_2(rideheight) = 108{,}8cm$ and the wand length is then calculated by equation 9 to be 142cm. This wand length will also leave about 50cm of centreboard in the water when the wand angle is at zero. In other words, it will be almost impossible for the boat to jump out of the water. H_2 is now described in equation 23. below

$$H_2 = 1{,}42 * \cos(\alpha_w) \quad \textbf{(23)}$$

This part can be made of Flax fibre, the characteristics of Flax fibre composites varies depending on the laminate design. An arbitrary cross section of the wand was calculated to use in this design. The force calculated in chapter 7.5 and the material data in table 2 was used to calculate a cross section that would not bend more than 10 mm at the end under this load (equation 4).

7.2.2 The Cam

Connected directly to the wand is the cam. This is where the non-linear nature of the wand and flap is modified to a linear lift behaviour.
The profile of the cam is then given in polar coordinates by using a base radius r and adding the desired distance, dr, for the system to travel at different ride heights, dr is the offset of the flap at a certain ride height. Which at the cam is the same as the horizontal distance travelled by the cam follower from the base radii. Thus, when no gain is implemented in the system $dr = x$. The function to plot the cam profile can now be described as equation 24.

$$r(\alpha_w) = r + dr(\alpha_w) \quad \textbf{(24)}$$

First, the base radius had to be decided. To investigate an optimal r equation 19 was used with F_c as described in equation 18. The torque transferred by the cam is now described by equation 25.

$$M_C = F_{out} * tan(\alpha_c) * r \quad \textbf{(25)}$$

This shows that the output torque will always benefit from a small base radius while the slope angle is kept small. To find an optimal r a differential equation must be solved and optimized since the slope angle is dependent of the radius. However, in this application of the cam an arbitrary picture shows that since the slope does not have any bends or kinks because of the linear behaviour suggested by Formula sailing the radius can be kept small throughout the range. However, if the slope angle exceeds 45 degrees the $tan(\alpha_c)$ component becomes larger than 1 and increases the torque rapidly. The base radius was kept at 100 mm which allows for some safety margin to the slope angle.

To further decide the profile of the cam equation 1 was used.
H can now be described as a function of the wand angle using equation 22 and 23

$$H = 1{,}42 * \cos(a_w) - 0{,}416 \quad \textbf{(26)}$$

α_f is also described in equation 15 and is inserted into equation 1 and replacing x with dr. Equation 27 is now retrieved.

$$sin^{-1}\left(\frac{dr}{L_f}\right) = -11{,}9 * (1{,}42 * \cos(a_w) - 0{,}416) + \boldsymbol{\alpha_{opt}} \quad \textbf{(27)}$$

Using $\alpha_{opt} = 2$ (Prabahar, 2020) and solving equation 27 for dr the general cam function is obtained, described in equation 28.

$$dr = L_f * \sin\left(11{,}9 * (L_w * \cos(\alpha_w) - 0{,}416) + 2\right) \qquad \textbf{(28)}$$

The cam profile could now be plotted using equation 24 with dr described in equation 28. Attachment 1 shows the code used to plot the cam profile in MatLab. Attachment 2 is the result of these calculations and shows the full relation between ride height and flap/wand angles these are plotted below in figure 7.2.

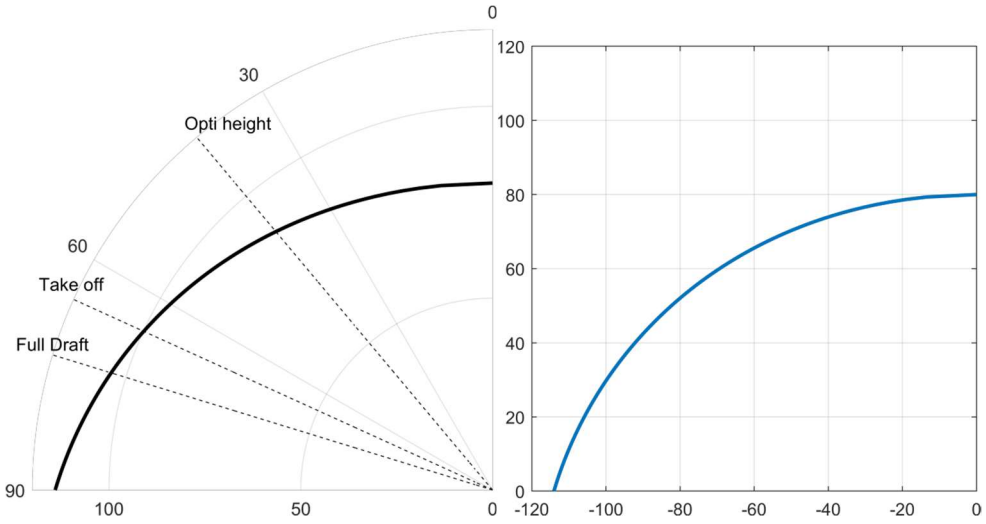

Figure 7.2 plot of the cam shape in polar and Cartesian coordinates. The lines in the left view, starting at the lowest one, represent cam position at full draft, take off and optimum ride height, respectively.

In this design the slope will be steepest at large wand angles. The largest change of slope per degree of the wand travelled is found just as α_w reaches 90 degrees. By taking the difference in radius at the first two pints in attachment 2 this can be estimated to a slope angle of the cam of 15 degrees. Inserting in equation 21 we get a resulting force that needs to work on the wand's end to keep the cam in a fixed position at the maximum possible output force 263 N :

$$F_{inMAX} = 5{,}5\ N$$

Which in this context is an improvement by 40% compared the Mach 2 solution which in the same scenario would provide 9 N force on the wands end. Further up the ride height this improvement becomes even larger since the cam slope angle decreases.

To allow increased stability for the boat when the boat is at full draft the cam should work linearly through the entire 90-degree span. This represents the extension of the arc in figure 7.2 to negative ride heights (beyond full draft). This is the scenario for the leeward wand when the boat heels at full draft.

7.2.3 Pushrods and pivot-points

The signal will be connected from the cam follower to the control box with two pushrods, angled at a pivot-point. The pushrod between the cam follower and the pivot-point is pushrod 1 and the one going inboard from the pivot-point is pushrod 2

The pushrods connecting the input signal to the rest of the system was dimensioned for buckling with equation 5. Pushrod 2 was dimensioned for its cross section since the length was decided. Pushrod 1 could be supported at several points. The distance between these supports was calculated with the same equation but with a set thickness. This shows that pushrod 2 needs a 7,2 mm diameter. The one attached to the cam follower will have the same diameter to save weight but because of its length it should be supported every 0.9 m, which in this design corresponds to one support halfway between the pivot-point and the cam follower.

The pivot-point turning the signal 90 degrees to go inboard from the racks will follow the design discussed in chapter 4. Its shafts need a diameter of at least 7,5 mm to withstand the shear forces applied by the rods.

7.2.4 Bellcrank

The bell-crank is the pivot between the vertical rods in the centreboard and pushrod 2. The crank also acts as a gearbox to enable changes in gain. As a starting point crank will have a 1:1 ratio but by changing the length from the pivot to the connection of pushrod 2 the ratio can be changed using equation 16.

The bell-crank will also feature the mechanism which enables the system to tack. This will be done by changing the position of the bell-crank shaft. To achieve the substantial lift difference and therefore a change in centre of lift described in chapter 2, a difference in flap angle of 4 degrees is required. Looking at the table in attachment 2 it becomes clear that a 4-degree difference in flap angle is translated to about 8 mm of travel in the system, since one is increasing while the other side is decreasing the shaft needs to travel 4 mm in each direction. This is described in 5.2.4c.

Another feature that can be integrated on the bell-crank is a weak-spot to make sure nothing breaks if loads are larger than expected. The weak-spot will then be located between the centreboard-pull rod and the bell-crank. This can be made in several ways; one is to have a weak pin connecting the parts that breaks under large loads, using the equation 8 for shear forces the material and dimensions of this pin can be found. Another solution is a ball-release system where a spring-loaded ball locks on to the pull-rod but releases when the load gets too high. The mathematics behind this is presented in figure 7.3 and equation 29.

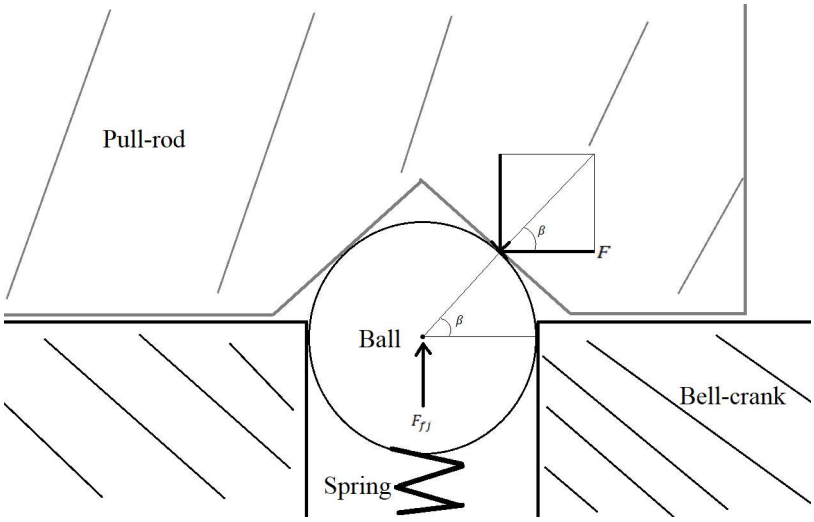

Figure 7.3, a simple version of a ball release system.

$$F_{fj} = F * \tan(\beta) \quad \textbf{(29)}$$

The groove in the pull rod should be spherical as well to not produce any excessive forces in the points of connection. This sketch was made simple to show the mathematics. In our case the force in the pull-rod is maximum 263 N, with the safety factor the dimensioning force 315 N. The ball should release at 315 N. Assuming a β of 20 degrees we get a spring force of ~115N. As soon as this force is reached the ball will start to move away, increasing F_{fj} linearly and β non-linearly with the travel of the ball. This results in a release. The spring will be adjustable so that if the system releases too often there is a possibility to increase the release force.

The bellcrank shown in figure 7.4 is the most complicated part in this system, it consists of two arms extending at a 95 degree angle from a pivot-point, The arm connecting to the pullrod should be 115 mm due to simplicity in design. The other arm should be 115 mm + 2*(1/10*115 mm) so that the gain can be decreased down to 0.83. If this gain is changed $dr \neq x$ and the foiling characteristics will change. This is therefor considered a tool for the sailors to enable change to the foiling characteristics while sailing. The bellcrank-connector has a diameter of 8 mm, therefore the base cross section of the arms is a 8*8 mm square.

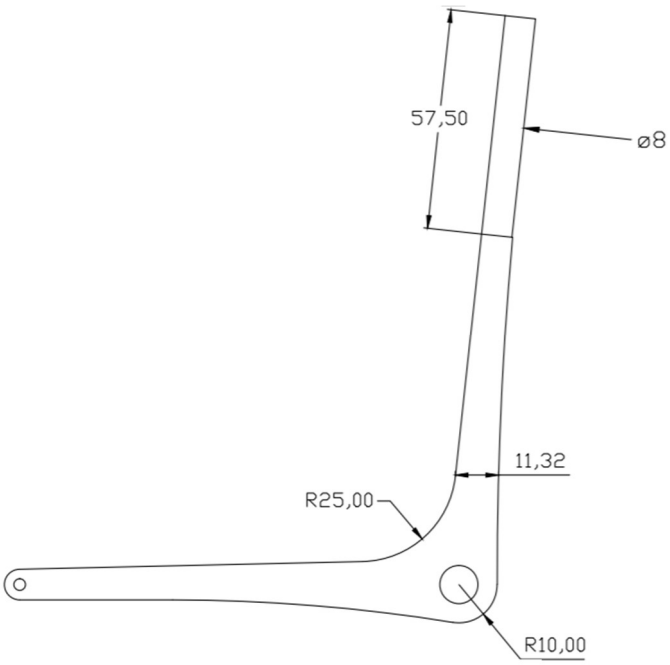

Figure 7.4 Sketch and important measures of the bellcrank

Because of the complexity of this part substantial computations was made on its strength. Equation 2 was used to find a cross section area for the two arms. Assuming each arm is a narrow beam fixed at one end with a force acting on the other end. Using a rectangular cross section with the base 8 mm the height of the rectangle needs to be at least 11,7 mm at the fixed point. Therefore, the beam needs to go from a square cross section to a rectangular one.
To investigate its strength where the arms meet the pivot a FEM analysis was made to ensure that the design does not provide stress in the connections which exceeds the properties of the material. The simulation and analysis tool in CATIA were used to simulate the load case. The maximum load was used at the staring position of the bellcrank-connector and at the pullrod fitting. The surface around the pivot axis was clamped in space to represent a static position. This is a the most extreme load case possible for the system. Several computations were made with smaller and smaller mesh sizes until the model converged at a parabolic tetrahedral mesh with size 5 mm and sag 1 mm with finer mech locally: size 1 mm and sag 0.1 mm to increase the accuracy where the stress concentrations occurred. During the analysis the importance of the radius where the arms meet the circular part of the part became clear. Without any radius a stress concentration is inevitable. The radius was increased and after a few runs it became clear that the arm needed to be thicker closer to the pivot to meet the increasing bending moment caused by the increased distance from where the force is acting just as the handbook calculations showed.

The analysis also pointed out that there was excess material around the pivot that could be removed without sacrificing strength. The result is displayed in figure 7.5 and shows the part under load. The colour corresponding to each Von-Mises stress level is displayed in the legend. The only critical area is where the square cross section is tapered to a cylindrical one. In this model the stress exceeds the materials yield-strength with 30MPa, but this can be neglected since this concentration appears in the taper between the square cross section and the circular.

This is considered a numerical error due to small edges which the mesh is too large for. The important areas of the part are well within the limits on this design. The exact dimensions of this part are not stated here but a simple sketch of the important measures is displayed in figure 7.5.

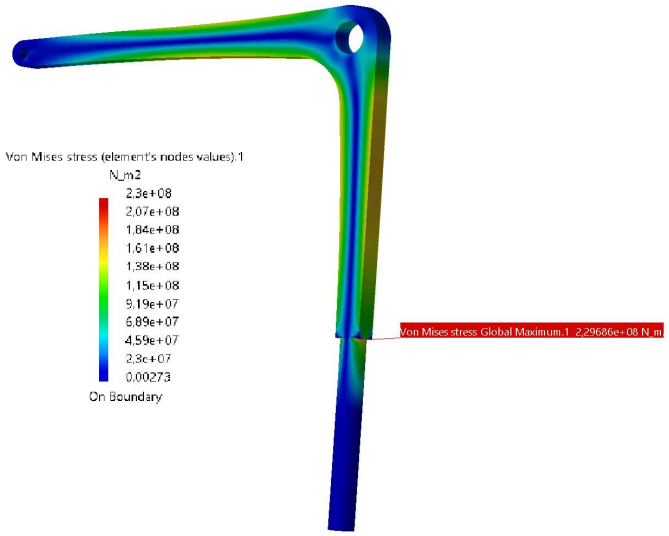

Figure 7.5 Static analysis of the bellcrank with its suggested shape. The Von-Mises stress along the beams are within the matelial yield-strength. The critical area is where the beam is tapered to a cylindrical shape (Pointed out in red).

7.2.5 Flap Connector

From the bellcrank, a pullrod will travel down inside the centreboard to connect to the flap lever. Measuring the geometry of the centreboard and if the walls of the foil are 5 mm thick the available space is 8 mm across the profile at the widest point. The distance from the foil and the deck in the design at this point is 1,94 m. The geometry allows for two pull rods, each 4 mm in diameter. To enable some play for the rods to move, 3 mm diameter rods with a circular cross section is the maximum possible. Using stainless steel with the characteristics in table 3 a minimum radius of the cross section is calculated with equation 3 to 0,57 mm. To allows for some negative forces without buckling the maximum rod size of 3mm possible is chosen.

The flap connection is the output of the system and will therefore be as important as the wand. To not put too much pressure into the system the lever that connects the flap to the pull-rod needs to be as long as possible. An optimal L_f was found at 115 mm when investigating the models of the foil. At 115 mm from the aft edge of the centreboard is where the widest point of the centreboard is, so to have the connection to the pull-rods here will give more space to design these rods. If the lever would be any longer the centreboard profile would get narrower and less space will be available, although it would provide a longer lever. If the geometry of the foil changes, L_f must change. This is also where the bellcrank's base length comes from, since it simplifies the design.

Looking at figure 7.2 the flap angle should be at its optimal 2 degrees at take-off. All other angles are interpolated with equation 1. The point where the rod connects will travel in y-direction (longitudinal) as well, but since the operating span for the flap is in between ±8 degrees this travel in y is always less than 1 mm and if the boat would reach the limits of its ride height range the travel in the y-direction will be maximum 1,756mm. This is less than 0,1% of the total rod length and the misalignment can therefore be neglected.

With a lever length of 115 mm the maximum force put on the system will be 263,3 N (316 including safety factor), the lever itself can then be dimensioned to not bend when under the maximum load. A I beam cross section will have the strongest strength to weight ratio for this part since it will only experience forces in one direction, but since the base is limited to only 4 mm, a rectangular cross section was chosen. Using equation 4 the height of the cross section of the beam can be calculated. The base is already at its maximum of 4 mm due to space limitations and the yield strength of stainless steel was used. The height is calculated to 16.5 mm.

To connect this lever to the rest of the flap an insert is suggested. (Breder, 2020) This means that the lever is connected to a flap-like shape on the other side of the pivot, which at the start is the same shape as the flap but 10 mm from the edge steps down 3 mm. The actual flap will then be able to slide on to this insert and glued in place, This solution is spreading out the load from the control system to a bigger area of the flap composite laminate. Exactly how far into the flap this insert goes is decided by the laminate in the flap's strength and not included in this report. The critical area is where the lever meets the flap, therefore significant radii on this connection was made and the model was then run through a FEM analysis. The loads wereapplied as a bearing-load where the pullrod connects and as a distributed load over the insert and the pivot was clamped in space. The model converged with a mesh consisting of parabolic tetrahedrals with a size of 2 mm and sag 0.5 mm, locally applied at the radii with a size of 0.2 mm. The radii were increased until the model met the materials constraints, resulting in radii of 3 mm alongside the beam and 7 mm at top and bottom. Figure 7.6 displays results of the FEM analysis with the corresponding stress level in the legend. Note that with these radii the largest stress concentrations are on the actual edge of the beam, not on the radius itself. This is probably caused by some computational error due to the small geometry at the edge and should not be a reason for failure of this part

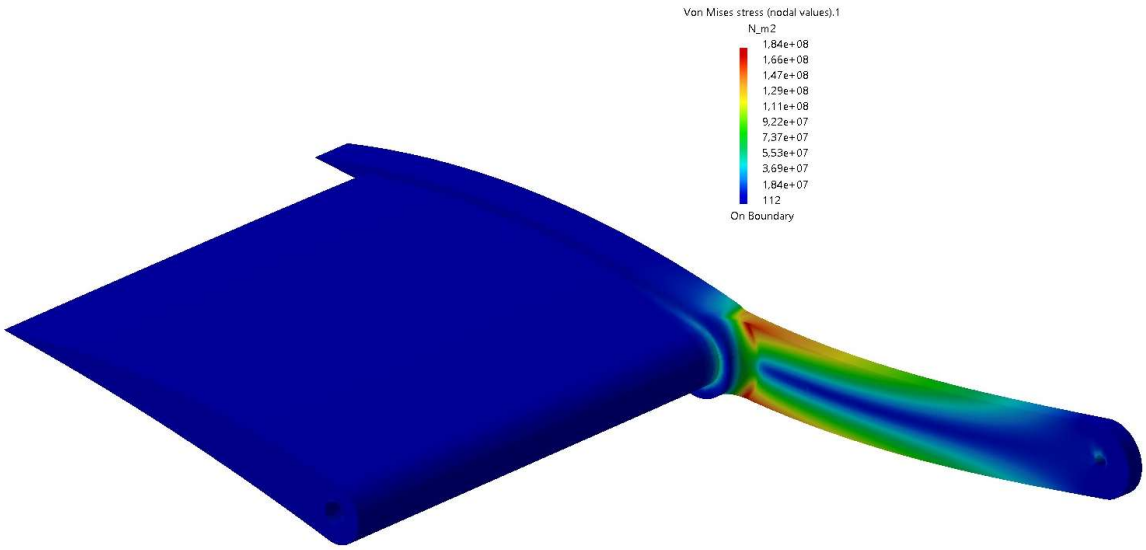

Figure 7.6 FEM static analysis of the flap lever. With this design all the stress levels are well within the limits of the material.

7.3 Final concept and models

This chapter will present the resulting control system of this project, part by part. Starting at the input at the wand and following the signal to the flap. No detailed drawings will be presented due to the project's limitations. Drawings must however be made at some point prior to manufacture. These are easily created from the now existing 3D models. Important aspects to the design that must be kept in mind during manufacture will be presented in a simple way to make future work easier.

7.3.1 The wand

Figure 7.7 shows the design of the wand. In this design the wand can be made of the same linen-cashew laminate as the hull, with a core of balsa, to make it as light as possible. At the end skimming the water a small paddle is fitted. This paddle is similar to the Mach2 design and is about 100 mm high and 50 mm wide. On the other end is the fitting to the cam. This is made by two M4 bolts going through the holes and are locked in place with nuts.

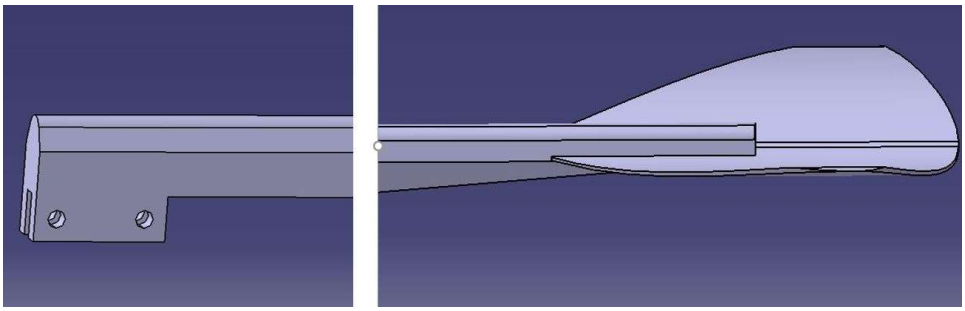

Figure 7.7, Design of the wand.

The cross section is dimensioned to not bend under the largest possible load. Using the characteristics of the linen-laminate the cross section shown in figure 7.8 gives an appropriate moment of inertia for the forces put on the wand.

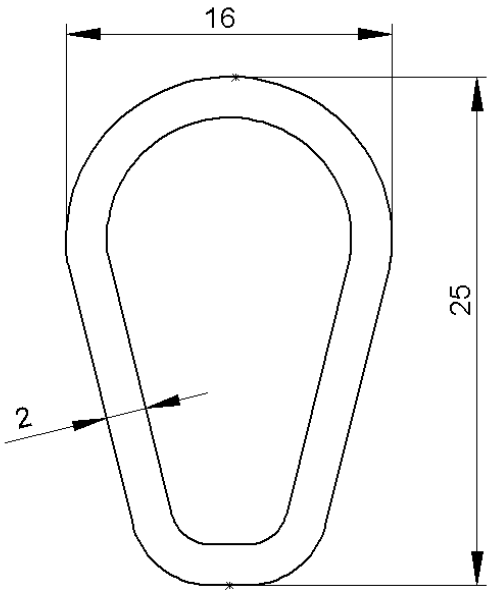

Figure 7.8 Suggested cross section of the wand.

This cross section is only a suggested design for this material and load scenario.

7.3.2 The Cam

The cam can be made of 3 mm stainless steel and shown in figure 7.9. The precision of its shape is very important. It is therefore suggested to cut this part with a CNC machine. At the pivot, reinforcements are made to avoid bending of the cam at its shaft. These can be fitted with bolts or welded. The cam is connected to it´s shaft with a set-screw. The arm extending up from the cam is to attach an elastic rope to the cam, which pushes the wand down into the water. At the right corner of the cam is a physical stop for the cam wheel, which stops the wand from rotating backwards too much. The two holes on which the wand connects are also visible.

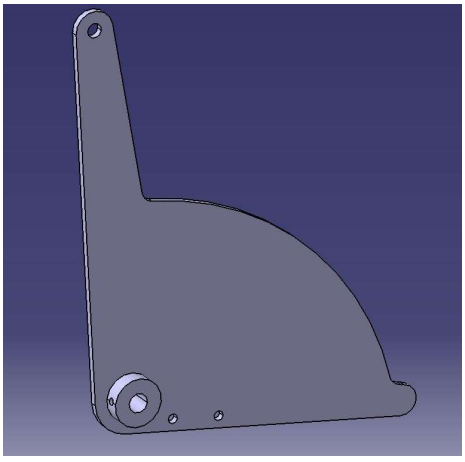

Figure 7.9, 3D render of the cam

The cam-shaft is a 8 mm stainless rod. It connects to the Cam-holder with two Teflon-bearings and is kept in place by a bolt and a washer. Rolling on the profile of the cam is the cam-wheel which is attached to the cam-follower. It is suggested to put the cam-wheel on a ball bearing since this wheel will travel a lot. The cam-follower is a plastic tube which connects to the first control rod. The follower's job is to stabilize the cam-wheel by sliding inside a tube with two Teflon-bearings as distances. The tube is connected to the racks. Figure 7.10 shows the assembly of these parts. Note that to get the measurement of ride height more accurate an extension of the rack is needed. It is suggested to extend the racks as far forward as possible. The existing design should therefore get a 1,3 m extension of the racks.

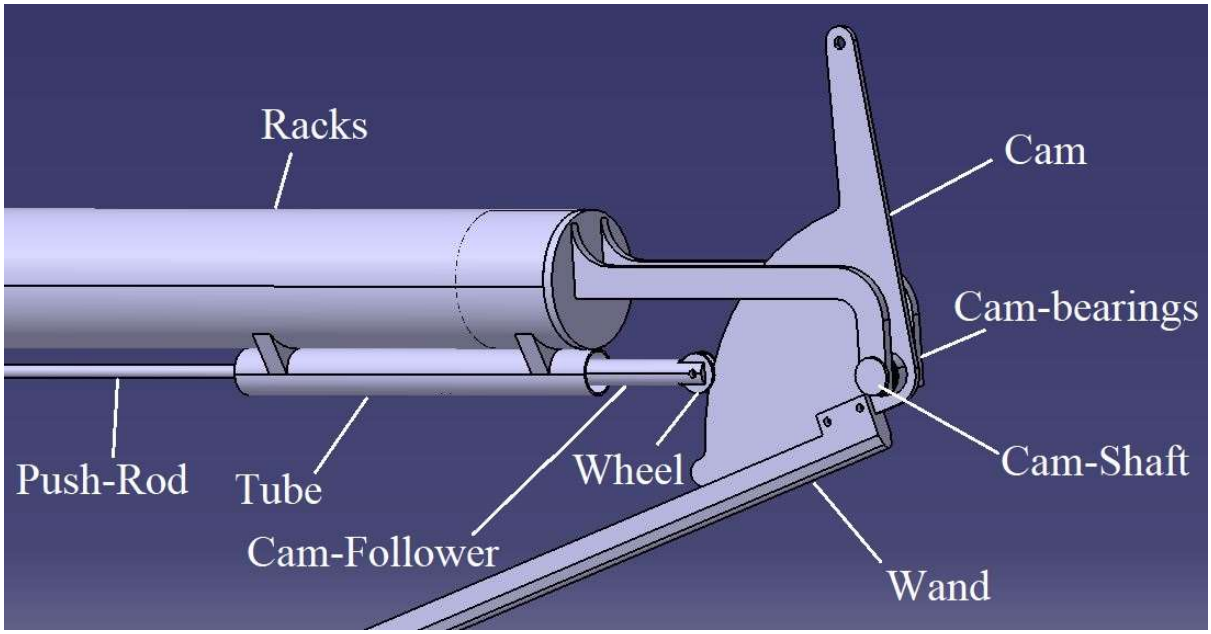

Figure 7.10, The assembly of the front racks.

Below in List 1 important aspects of this design is presented that should be kept in mind in manufacturing.

List 1

- The cam pivot must be at the same level as the cam follower. If these don't line up the cam design is no longer accurate.
- The profile of the cam is very important and should be calculated and manufactured carefully.
- To lubricate moving parts Teflon-bearings are suggested, except for the cam-wheel. This should be on a ball bearing, which needs to be lubricated regularly.

7.3.3 Pushrods and pivot point

Both pushrods will have a threaded end to precisely set their lengths. Figure 7.11 shows pushrod 1's threaded connection to the cam follower.

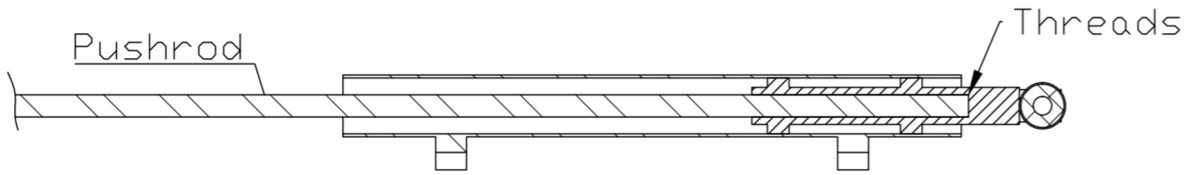

Figure 7.11 Cross section of Pushrod 1's connection to the cam follower inside the tube guiding and supporting the follower.

The connection to the control box is made in a similar way but with a part called the "Bellcrank-connector", which will be described in the next chapter. Figure 7.12 shows a cross section of this connection.

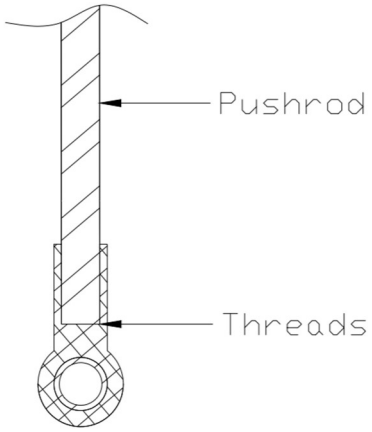

Figure 7.12 Pushrod 2's connection to the bellcrank-connector.

The pivot-point will be attached to a bracket which attaches to the underside of the rack. It will be positioned so that pushrod 1 is parallel to the rack both vertically and laterally and pushrod 2 is perpendicular to the rack going inboard. Figure 7.13 shows a 3D render of the pivot-point attached to the rack from below. In this figure the screws holding it together are not included. The pivot-plate itself should be attached to its centre M8 bolt with a Teflon bushing and a spacer to decrease friction. The pushrods will be connected to the pivot-plate with M6 bolts and nuts.

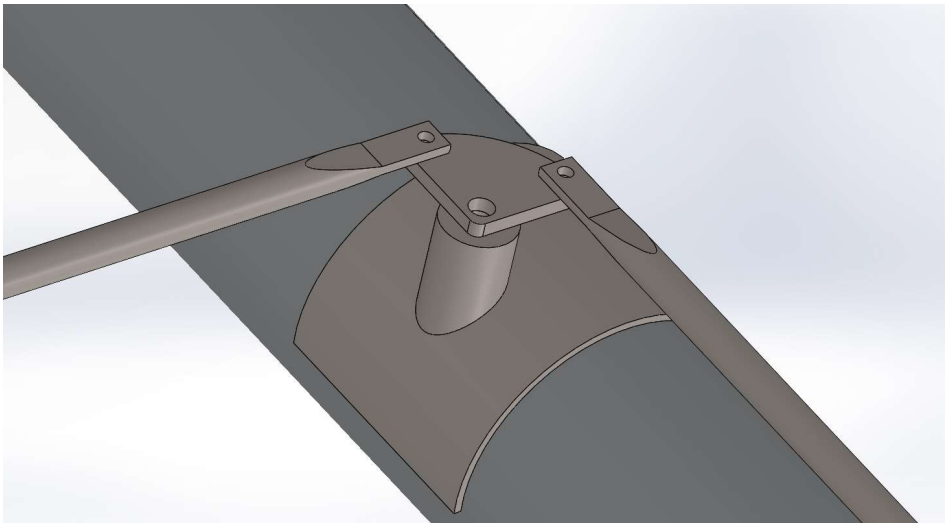

Figure 7.13 3D render of the pivot-point, pushrod 1 at the right connects to the pivot-plate transferring the signal to pushrod 2 on the left. Bolts and nuts are not shown.

A Mach 2 style offset screw will be positioned on pushrod 2 between the pivot-point and the control box to enable changes to the ride height between races. This screw can be custom made or bought off shelf from a Moth dealer (Sailing Bits, 2020).
The important design features of this assembly are listed in List 2.
List 2

- The rod should be assembled so that they are perpendicular when the flap angle is zero. This provides the least amount of misalignment through the range.
- The exact length of each rod has large tolerances since they both can be adjusted in one end.
- All parts must be made in stainless steel.
- Teflon bearings are suggested at the pivot-point while where the rods connect the surfaces are very small. Therefore, lubrication with grease should be sufficient.

7.3.3 The bell-crank and performance mode system

The bellcrank is a crucial part to the system and can be made by welding pieces of metal bars together or by cutting it out of a thick metal plate. Figure 7.14 shows the shape of the bellcrank with the parts connecting on each end.

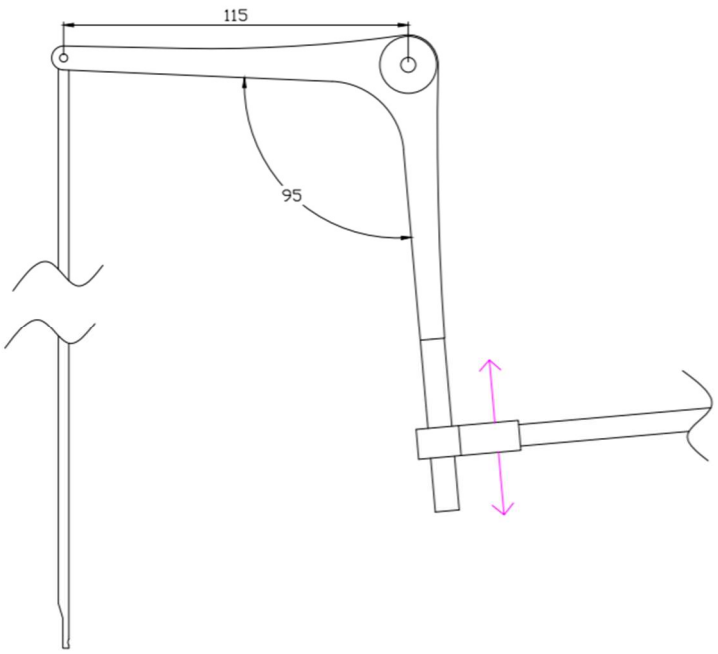

Figure 7.14 shows the Shape of the bellcrank with the bellcrank connector on the right and the pullrod on the left.

To adjust for the angle on which pushrod 2 has, going from the racks, the bellcrank needs to have a 95-degree angle between its arms. Pushrod 2 connects to one arm via the bellcrank-connector which can be adjusted up and down on the bellcrank's arm allowing a change in gain. Changing this will cause some misalignment on pushrod 2 but the angles will be very small and therefore neglected. This movement of the connector will be made by having two nuts on the bellcrank arm, one on each side of the connector. This connector can be bought off shelf as a rod end bearing, (Igus, 2020) with a diameter of 8 mm or the part can be custom made. At the end of the other arm, which in this design is the same length as the flap lever is where the pull-rod from the flap connects and where the possible weak spot is connected. The length of the bell cranks arms can differ from the 115 mm suggested, but they should be kept long so that the changes in gain can be made precisely. The bellcrank then pivots around a 5 mm shaft supported on both sides.

It is the design at this shaft that allows for a pivot-point offset, which enables the system to be put into performance mode. The bellcrank's pivot-point will be mounted on the walls of a control box that is fixed to the boat deck. This box supports the bellcrank and the performance bracket. Figure 7.15 shows a 3D render of this design with the important parts pointed out.

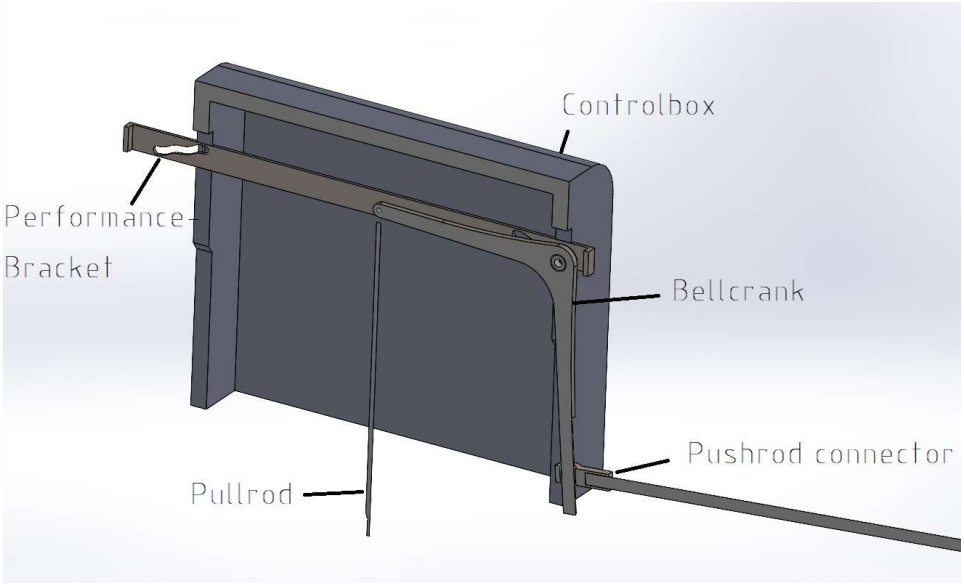

Figure 7.15 Cross section of the control box and its contents on one side. In reality the pullrod will be much longer extending down into the centreboard and there will be a bellcrank fitted on the other side as well.

By having the shaft supported sideways by the walls of a groove in the control box and supported up and down by the performance bracket that can slide sideways. The groove in the performance bracket is shaped so that it changes the height of the shaft by 4 mm depending on which sideways position the bracket is in. 7.16 shows a section view where the two tracks are visible.

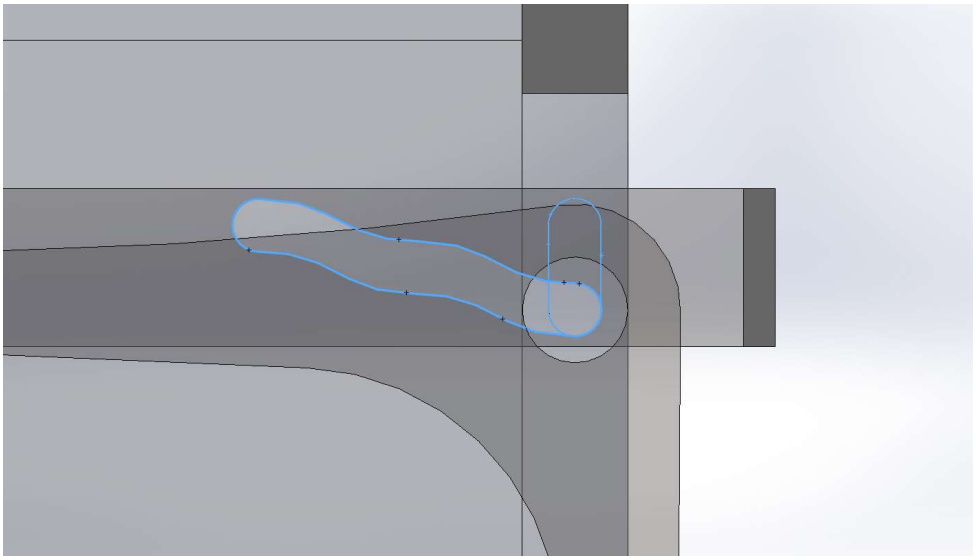

Figure 7.16 Section view of the control box with the bellcrank and performance bracket shaded. Highlighted in blue are the two tracks allowing the change in vertical position of the bellcrank shaft.

The 4 mm of vertical displacement is made by sliding the performance bracket 15 mm sideways between each step. The groove on the other side of the bracket is mirrored about its centre, therefore if the shaft is moved up 4 mm on the starboard side at the same time it moves down 4 mm on port. This will give the sailors one performance mode for each tack and one “neutral”

mode. The bracket should be CNC cut out of 2 mm stainless steel sheet to ensure the shape of the track is precise. Figure 7.17 shows a suggested design for this part.

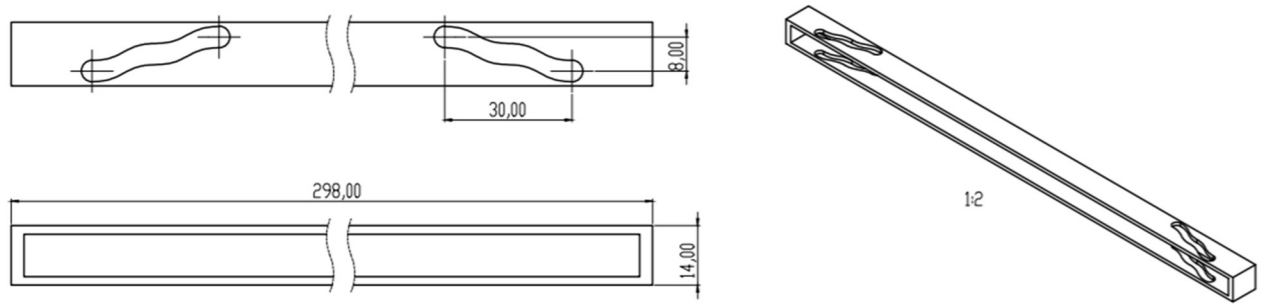

Figure 7.17 Suggested design for the performance bracket. Bottom left, top view. Upper left side view. Right, Isometric view.

To enable control of the performance bracket while sailing a rope can be attached to the side of it which extends out to the rack, then the rope should be threaded into a loop by going to the racks on the other side and finish at the other end of the bracket. In that way the mode can be changed in both ways with one rope. The reason to have exactly 15 mm between the modes sideways is because an automatic snap back can be implemented. By mounting another rope or wire attached between pushrod 2 and the end of a bracket with a precise length the bracket will snap back to neutral when the boat drops down into the water from foiling in performance mode, giving the sailors one less setting to think about when getting back up on the foils. The performance mode can then be engaged again manually.

There is a lot of freedom in the design of the control box, but it should be made so that it takes up as little space at possible at the same time managing to suspend the bellcrank firmly. The box can be made of the same flax composite as the hull to save non-organic weight. In that case reinforcements in stainless steel will have to be inserted to the track for the bellcrank-shaft. To decrease friction in these parts they should be lubricated regularly. The bellcrank should slide on its shaft with a Teflon bearing. The surfaces between the shaft and the tracks should not be lubricated to avoid slip.

7.3.4 Connecting the flap

Figure 7.18 shows a 3D render of the suggested flap insert which connects the system to the flap of the foil

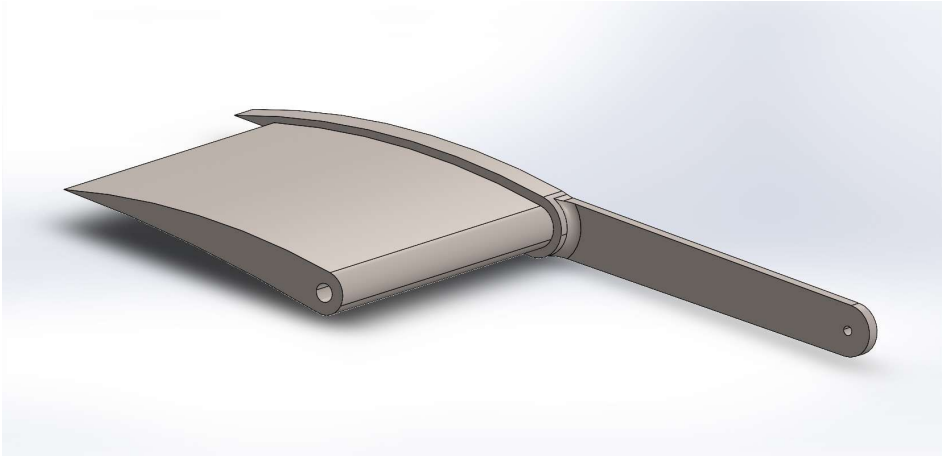

Figure 7.18 The insert for the flap connection. The pullrod connects to the lever on a shaft to the right. Torque is then transferred over the pivot to the flap insert. The distance between the two shafts is 115 mm.

The final shape of the flap lever will have to be discussed with the designers of the rest of the foil, to make sure no losses in hydrodynamics are made due to the space the lever will require. The FEM analysis shows that the insert can be made hollow to save weight, but this will have to be developed together with the structural designers of the flap laminate.

7.3.5 Setting up the system.

To set up the system is easy, first set the wand at ~65 degrees and make sure the cam wheel is in contact with the cam, then pushrod 1 can be turned 0,5 turns at a time to make sure that the pivot-plate is perpendicular. Make sure that the bellcrank is in its starting point and the connector is at 1:1 ratio height. Then rotate the offset screw until pushrod 2 can be connected to the pivot-plate. Do the same procedure at the other side of the system, finally measure the angle of the flap at this wand angle and make sure it is 0 degrees by fine tuning the offset screws. If a lot of adjusting is required to achieve this, the pullrods inside the centreboard have the wrong length and need to be replaced. Now the boat is ready to fly.

To install the automatic drop back system, a thin stiff rope would have to be attached to the performance bracket going out to a block on the rack and then attaching at the offset screw. Then this rope needs to be set to the correct length so that it pulls the bracket to neutral when the boat is low enough in the water. This will probably require some fine tuning to make it work properly.

8 Discussion and future work

Throughout this thesis a lot of different options on how to control flight for a dinghy were considered. I believe that this system has the features and stability to provide a foiling experience never experienced before (Boman, 2019). Although there will always be improvements. First off, the passive heel control on this system is a compromise between simplicity and performance. At this point no logical solutions on how to decouple the heel from the height mechanically was found. The solutions which the team brainstormed was either too complicated or too heavy to improve the system's performance. This system will make the boat fly more stable than what would ever be possible with a single flap and the performance mode allows for manual control of the stability, which can be experimented with by the sailors. But an active heel response would be better for performance. Then a cam design which looks more like "Bug's" can be used so that the optimal flap angle can be kept longer during take-off and with a more distinctive high flight zone. Adding in to that an active heel response can be made more aggressive to prevent heeling even more. A lot of future work can go into designing the optimal cam to increase the boats performance.

At one point in the beginning of this project an auto-tacking performance mode was considered. This idea was based on the jib traveling from one side to another on the jib-track when the boat changes tacks, and using that force to change the side of the performance mode. But this would add a lot of parts to the system, and since the boat is made to sail in light winds there would not be sufficient force on the jib-car going through the tack. It would most likely result in the jib being stuck in the middle of the boat and with the system still on the wrong tack. Therefore, the auto-drop back was introduced, so that if something goes wrong and the boat drops back into the water the system will be put back into neutral.

Since this thesis was made only from a control system point of view there are some aspects of the hydrodynamics and structures of the foil that have not been thought of. For example, the shape of the wand has only been suggested and should be further investigated to provide a large lift with low drag. How much space there is where the flap-lever is supposed to be will most likely be a compromise between the hydrodynamic sacrifice and the length of this lever. Also, the size of this lever will be dependent on how much space is left after the structures of the foil has been decided. But the control system must work properly if the boat will be able to fly at all and therefore sacrifices in other areas will probably be made. Throughout this project the method used was evaluated with Formula Sailing. Discussions weather it would be possible to test prototypes or ideas on the boat itself could have given a more precise concept, but access to the boat was very limited during this time. It was decided that a virtual model of the concept would be sufficient to continue working on. That also makes the next step in a building process very clear, constructing prototypes.

It was mentioned in the thesis that larger craft use hydraulics. This would solve a lot of issues with this system. It would probably be lighter and at the same time be able to manage larger forces which means that the flap lever can be shorter and the structures where the centreboard meets the foil can be smaller. But at this point no hydraulic system of the right size was found.

However, if a supplier is found in the future a hydraulic system is easily implemented in this design. Simply change the pushrods for hydraulic tubes, and if space is provided even the pullrod inside the centreboard can be changed.

As an elite sailor the complexity and difficulty to make a two man dinghy of this size fly was at first an appalling thought, but with the split flap system things seemed slightly more manageable. There is no doubt that it will still take a lot of practice to fly this boat around a track, but I believe that with this system and the tools given to the sailors to control the system for their needs it will be possible to achieve great results, with enough practice.

References

1001Vela Cup. (2019, 09 19). *1001Vela Cup regolamento*. Retrieved from 1001Vela Cup: http://www.1001velacup.eu/regolamento/regolamento-di-classe.html

Acerbi, T., Andersson, R., Eriksson, E., Granli, S., Jacobs, E., Rita, F., . . . Werner, E. (2017). *Chalmers Formula Sailing.* Gothenburg: Chalmers.

Bethwaite, F. (2008). *Higher Performance Sailing: Faster Handling Techniques.* Adlard Coles Nautical.

Boman, A. (2019, 09 05). Own Experience. (A. Boman, Interviewer)

Breder, J. (2020, 02 07). Private conversation. (A. Boman, Interviewer)

'Bugs' Smith, P. (2019, 09 27). *Avalon Sails Blog*. Retrieved from Bugs Cam: https://avalonsails.com.au/blog

CEC Catamarans. (2019, 09 13). *iFlySail*. Retrieved from https://iflysail.com/

Dackhammar et al, P. (2018). *En flygande kappseglingsjolle.* Gothenburg: Chalmers University of Technology.

Dahlberg, T. (2001). Formelsamling i hållfasthetslära. In D. Tore, *Teknisk Hållfasthetslära* (p. 30). Göteborg: Studentlitteratur.

Foiling Week. (2020, 10 31). *Foiling Week*. Retrieved from Foiling Week: https://www.foilingweek.com/

FormulaSailing. (2019, 10 -). Brainsorming sessions. (A. Boman, Interviewer)

hartasproductions. (2020, 04 03). *The mothclass is all about innovating...check out this articulated and! [Instagram photograph].* Retrieved from https://www.instagram.com/p/B-gs0sKjCLO/?igshid=59xlpyy9merl.

Igus. (2020, 02 04). *Igus*. Retrieved from Spherical bearings: https://www.igus.eu/igubal/polymer-spherical-bearing?sort=3&fc=300730&inch=false&minshaftdiam=8&igubconsize=7

Larsson, L. (2019, 09 -). Supervisor. (A. Boman, Interviewer)

Libo, Y., Nawawi, C., & Krishnan, J. (2013). Flax fibre and its composites – A review. *Elsevier Ltd.*, 308.

McDougall McConaghy. (2019, 09 13). *Mach2.5 3D*. Retrieved from Mach2.

Prabahar, N. S. (2020, 9-12). Personal comunication. (A. Boman, Interviewer)

Pugh, S. (1990). *Total design : integrated methods for successful product engineering.* Wokingham: Addison-Wesley.

Sailing Bits. (2020, 02 04). *Sailing Bits*. Retrieved from Mach 2.3 Ride Height Adj Barrel: https://sailingbits.com/class-specific/moth/mach-2/control-systems/mach-2-3-ride-height-adj-barrel/

Schmidt., D. (2007). Learning to fly. *Sail Magazine*. Retrieved from https://www.sailmagazine.com/racing/learning-to-fly-2

Zienkiewicz, O., C. Taylor, R., & L. Zhu, J. Z. (1991). *Finite Element Method Its Basis & Fundam.* Elsevier Science & teknik.

Attachments

Attachment 1

MatLab code used to plot the cam profile

```
close all
clear
clc

%% Inputs
r  = 100;                                                % Cam base Radius in mm
Lw = 1420;                                               % Wand Length in mm
Lf = 115.64;

height = 0:20:1420;                                      % Height
alfa_w = acosd(height./ Lw);                             % Wand Angles based on the
height
alfa_f = -11.9225 * (height  - 416.814) * 1e-3 + 2;      % Flap Angles based on the
(Ride height = height - 416.814)
x      = Lf .* sind(alfa_f);                          % Cam travels from the base
radius

alfa_w_zd = acosd(416.814 ./ 1420);                      % Wand angle at Full Draft
alfa_w_tf = acosd(587.814 ./ 1420);                      % Wand angle at Zero Draft
alfa_w_mx = acosd((587.814 + 500) ./ 1420);              % Wand angle at 0.5 m Ride
Height

cam_profile = x + r;                                     % Cam profile

%% Slope Angle 'alfa_C' at every instant of wand angle 'alfa'
for i = 1:length(cam_profile)-1
    slope(i) = atand((x(i+1) - x(i)) / (cam_profile(i) * tand(alfa_w(i+1) -
alfa_w(i))));
end

%% CAM profile in Cartesian Coordinates
for i = 1:length(cam_profile)
    XCar(i) = - cam_profile(i) * cosd(90 - alfa_w(i));
    YCar(i) = cam_profile(i) * sind(90 - alfa_w(i));
end

%% Plotting the polar CAM profile
% Angles should be in Radians, thats why the 0.0174533

ax = polaraxes;
hold on
polarplot(ax, alfa_w .* 0.0174533, cam_profile, 'LineWidth', 2, 'Color', [0 0 0])
polarplot(ax, [alfa_w_zd * 0.0174533 alfa_w_zd * 0.0174533], [0 r + 20], '--k')
polarplot(ax, [alfa_w_tf * 0.0174533 alfa_w_tf * 0.0174533], [0 r + 20], '--k')
polarplot(ax, [alfa_w_mx * 0.0174533 alfa_w_mx * 0.0174533], [0 r + 20], '--k')
text(ax, alfa_w_zd * 0.0174533, r+30, 'Full Draft')
text(ax, alfa_w_tf * 0.0174533, r+30, 'Take off')
text(ax, alfa_w_mx * 0.0174533, r+25, 'Opti height')
ax.ThetaDir = 'counterclockwise';
ax.ThetaZeroLocation = 'top';
thetalim([0 90])
hold off

%% Plotting the CAM profile in Cartesian Coordintates
figure(2)
```

```
plot(XCar, YCar, 'LineWidth', 2)
axis equal
xlim([-120 0])
ylim([0 120])
```

Attachment 2

Table generated by the Cam Profile Calculation.

r = 100							
Height	Ride Height	Wand Angles	Flap Angles	x	Cam Profile (r + x)	Cartesian - X	Cartesian - Y
0	-416,814	90,00	6,97	14,032	114,032	-114,032	0,000
20	-396,814	89,19	6,73	13,554	113,554	-113,543	1,599
40	-376,814	88,39	6,49	13,076	113,076	-113,031	3,185
60	-356,814	87,58	6,25	12,598	112,598	-112,497	4,758
80	-336,814	86,77	6,02	12,119	112,119	-111,941	6,317
100	-316,814	85,96	5,78	11,640	111,640	-111,363	7,862
120	-296,814	85,15	5,54	11,161	111,161	-110,764	9,394
140	-276,814	84,34	5,30	10,682	110,682	-110,143	10,912
160	-256,814	83,53	5,06	10,203	110,203	-109,501	12,417
180	-236,814	82,72	4,82	9,724	109,724	-108,838	13,909
200	-216,814	81,90	4,58	9,244	109,244	-108,155	15,386
220	-196,814	81,09	4,35	8,764	108,764	-107,451	16,851
240	-176,814	80,27	4,11	8,284	108,284	-106,726	18,302
260	-156,814	79,45	3,87	7,804	107,804	-105,982	19,739
280	-136,814	78,63	3,63	7,324	107,324	-105,217	21,162
300	-116,814	77,80	3,39	6,844	106,844	-104,432	22,573
320	-96,814	76,98	3,15	6,363	106,363	-103,627	23,969
340	-76,814	76,15	2,92	5,882	105,882	-102,803	25,352
360	-56,814	75,31	2,68	5,402	105,402	-101,958	26,722
380	-36,814	74,48	2,44	4,921	104,921	-101,094	28,077
400	-16,814	73,64	2,20	4,440	104,440	-100,211	29,420
420	3,186	72,80	1,96	3,959	103,959	-99,308	30,748
440	23,186	71,95	1,72	3,478	103,478	-98,385	32,064
460	43,186	71,10	1,49	2,997	102,997	-97,443	33,365
480	63,186	70,24	1,25	2,516	102,516	-96,481	34,653
500	83,186	69,38	1,01	2,035	102,035	-95,500	35,928
520	103,186	68,52	0,77	1,554	101,554	-94,499	37,189
540	123,186	67,65	0,53	1,072	101,072	-93,479	38,436
560	143,186	66,77	0,29	0,591	100,591	-92,439	39,670
580	163,186	65,89	0,05	0,110	100,110	-91,378	40,890
600	183,186	65,01	-0,18	-0,371	99,629	-90,298	42,097
620	203,186	64,11	-0,42	-0,853	99,147	-89,197	43,290
640	223,186	63,21	-0,66	-1,334	98,666	-88,077	44,469
660	243,186	62,30	-0,90	-1,815	98,185	-86,935	45,635
680	263,186	61,39	-1,14	-2,296	97,704	-85,772	46,788
700	283,186	60,46	-1,38	-2,777	97,223	-84,589	47,927
720	303,186	59,53	-1,61	-3,259	96,741	-83,383	49,052
740	323,186	58,59	-1,85	-3,740	96,260	-82,156	50,164

740	323,186	58,59	-1,85	-3,740	96,260	-82,156	50,164
760	343,186	57,64	-2,09	-4,221	95,779	-80,907	51,262
780	363,186	56,68	-2,33	-4,702	95,298	-79,634	52,347
800	383,186	55,71	-2,57	-5,182	94,818	-78,338	53,418
820	403,186	54,73	-2,81	-5,663	94,337	-77,018	54,476
840	423,186	53,73	-3,05	-6,144	93,856	-75,673	55,521
860	443,186	52,73	-3,28	-6,624	93,376	-74,303	56,552
880	463,186	51,70	-3,52	-7,105	92,895	-72,907	57,569
900	483,186	50,67	-3,76	-7,585	92,415	-71,483	58,573
920	503,186	49,62	-4,00	-8,065	91,935	-70,030	59,563
940	523,186	48,55	-4,24	-8,545	91,455	-68,548	60,541
960	543,186	47,46	-4,48	-9,025	90,975	-67,035	61,504
980	563,186	46,36	-4,71	-9,505	90,495	-65,489	62,454
1000	583,186	45,23	-4,95	-9,984	90,016	-63,909	63,391
1020	603,186	44,08	-5,19	-10,464	89,536	-62,293	64,315
1040	623,186	42,91	-5,43	-10,943	89,057	-60,637	65,225
1060	643,186	41,71	-5,67	-11,422	88,578	-58,941	66,122
1080	663,186	40,49	-5,91	-11,901	88,099	-57,200	67,005
1100	683,186	39,23	-6,15	-12,379	87,621	-55,411	67,875
1120	703,186	37,93	-6,38	-12,858	87,142	-53,570	68,732
1140	723,186	36,60	-6,62	-13,336	86,664	-51,671	69,575
1160	743,186	35,22	-6,86	-13,814	86,186	-49,710	70,406
1180	763,186	33,80	-7,10	-14,291	85,709	-47,679	71,223
1200	783,186	32,32	-7,34	-14,769	85,231	-45,569	72,026
1220	803,186	30,78	-7,58	-15,246	84,754	-43,370	72,817
1240	823,186	29,16	-7,81	-15,723	84,277	-41,067	73,594
1260	843,186	27,46	-8,05	-16,200	83,800	-38,644	74,358
1280	863,186	25,66	-8,29	-16,676	83,324	-36,077	75,109
1300	883,186	23,72	-8,53	-17,152	82,848	-33,333	75,847
1320	903,186	21,63	-8,77	-17,628	82,372	-30,365	76,571
1340	923,186	19,32	-9,01	-18,103	81,897	-27,100	77,283
1360	943,186	16,72	-9,25	-18,579	81,421	-23,418	77,981
1380	963,186	13,63	-9,48	-19,053	80,947	-19,077	78,666
1400	983,186	9,63	-9,72	-19,528	80,472	-13,458	79,339
1420	1003,186	0,00	-9,96	-20,002	79,998	0,000	79,998

Department of mechanics and maritime sciences
CHALMERS TEKNISKA HÖGSKOLA
Göteborg, Sverige 2020
www.chalmers.se

CHALMERS